USAARL REPORT NO. 83-5

ANALYSIS OF IMAGE SMEAR IN CRT DISPLAYS DUE TO SCAN RATE AND PHOSPHOR PERSISTENCE

By
Clarence E. Rash
Sensory Research Division

and

Jacob Becher
Old Dominion University
Norfolk, Virginia

DTIC
ELECTE
MAY 0 1 1990
S E D

October 1982
U.S. ARMY AEROMEDICAL RESEARCH LABORATORY
FORT RUCKER, ALABAMA 36362

90 05 01 019

USAARL

AD-A221 095

NOTICE

Qualified Requesters

Qualified requesters may obtain copies from the Defense Technical Information Center, Cameron Station, Alexandria, Virginia. Orders will be expedited if placed through the librarian or other person designated to request documents from the Defense Technical Information Center.

Change of Address

Organizations receiving reports from the US Army Aeromedical Research Laboratory on automatic mailing lists should confirm correct address when corresponding about laboratory reports.
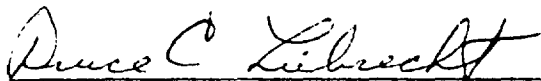
Disposition

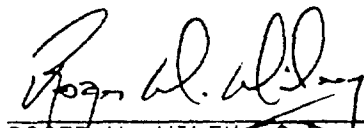Destroy this report when it is no longer needed. Do not return it to the originator.

Disclaimer

The views, opinions, and/or findings contained in this report are those of the authors and should not be construed as an official Department of the Army position, policy, or decision, unless so designated by other official documentation. Citation of trade names in this report does not constitute an official Department of the Army endorsement or approval of the use of such commercial items.

Reviewed:

BRUCE C. LEIBRECHT, Ph.D.
MAJ, MSC
Director, Sensory Research Division   Released for Publication:

ROGER W. WILEY, O.D., Ph.D.   DUDLEY R. PRICE
LTC, MSC   COL, MC
Chairman, Scientific Review Committee   Commanding

REPORT DOCUMENTATION PAGE		READ INSTRUCTIONS BEFORE COMPLETING FORM
1. REPORT NUMBER USAARL Report No. 83-5	**2. GOVT ACCESSION NO.**	**3. RECIPIENT'S CATALOG NUMBER**
4. TITLE (and Subtitle) ANALYSIS OF IMAGE SMEAR IN CRT DISPLAYS DUE TO SCAN RATE AND PHOSPHOR PERSISTENCE		**5. TYPE OF REPORT & PERIOD COVERED** Final Report
		6. PERFORMING ORG. REPORT NUMBER
7. AUTHOR(s) Clarence E. Rash Jacob Becher		**8. CONTRACT OR GRANT NUMBER(s)**
9. PERFORMING ORGANIZATION NAME AND ADDRESS US Army Aeromedical Research Laboratory Fort Rucker, AL 36362		**10. PROGRAM ELEMENT, PROJECT, TASK AREA & WORK UNIT NUMBERS** 64207.A,4E464207D425, 00,048
11. CONTROLLING OFFICE NAME AND ADDRESS US Army Medical Research & Development Command Fort Detrick Frederick, MD 21701		**12. REPORT DATE** October 1982
		13. NUMBER OF PAGES 47
14. MONITORING AGENCY NAME & ADDRESS(if different from Controlling Office)		**15. SECURITY CLASS. (of this report)** Unclassified
		15a. DECLASSIFICATION/DOWNGRADING SCHEDULE
16. DISTRIBUTION STATEMENT (of this Report) Approved for public release; distribution unlimited.		
17. DISTRIBUTION STATEMENT (of the abstract entered in Block 20, if different from Report)		
18. SUPPLEMENTARY NOTES		
19. KEY WORDS (Continue on reverse side if necessary and identify by block number) image smear scan rate phosphor persistence cathode-ray-tube		
20. ABSTRACT (Continue on reverse side if necessary and identify by block number) See back of form.		

DD ₁ FORM JAN 73 **1473**   EDITION OF 1 NOV 65 IS OBSOLETE

20. ABSTRACT:

The increase in the use of cathode-ray-tube (CRT) displays for target detection and recognition has placed an emphasis on the ability of these displays to accurately reproduce amplitude and phase information for dynamic targets. This analysis investigates the theoretical dynamic image degradation occurring at the display as a result of the interaction between the target/sensor relative velocity, the CRT system scan rate, and the persistence of the display phosphor. Expressions are developed to allow comparison of phosphors on the basis of modulation loss due to target/sensor motion. A model is developed which equates a target having a spatial frequency (S) and moving with a horizontal speed (V) to a stationary target with a sinusoidal varying intensity of frequency, f_t, equal to SV. The model identifies phosphor persistence as a major contributor to amplitude modulation loss and predicts several image artifacts such as "freezing" and apparent motion reversal.

PREFACE

Accession For	
NTIS GRA&I	☒
DTIC TAB	☐
Unannounced	☐
Justification	
By	
Distribution/	
Availability Codes	

Dist	Avail and/or Special
A-1	

---

* This report is the first part of a planned three-phase study of image degradation in cathode-ray-tube displays due to image motion. This first phase is a preliminary theoretical analysis of the problem; the development of a measurement system to quantify the amount of degradation will be the second phase; and the final phase will be an investigation of the psychophysics involved in viewing dynamic imagery on cathode-ray-tubes.

1

TABLE OF CONTENTS

Page No.

TABLE OF CONTENTS (Cont)

LIST OF ILLUSTRATIONS

LIST OF ILLUSTRATIONS (Cont)

LIST OF TABLES

INTRODUCTION

Despite continuing efforts in the development of newer display technologies, e.g., liquid crystal and electroluminescence displays, the center of most military, as well as commercial, video information transfer systems remains the Cathode-Ray-Tube (CRT). For this reason, a multitude of studies have been conducted to investigate the influence of various display parameters, e.g., display size, signal-to-noise ratio, video bandwidth, scan rate, resolution, and contrast, etc., on user performance. A comprehensive review of the most notable of these studies was compiled by Farrell and Booth (1975). The major purpose of the majority of these studies was to investigate the effects of the various electro-optical imaging system parameters on the user's ability to interpret the displayed information.

The current major military application of CRT displays is target search, detection, and recognition. The CRT aids in this mission by reconstructing a visual image of a scene which is being surveyed by a sensor which extends the capabilities of the human visual system. Such a sensor may extend the user's senses over an increased distance or into different regions of the energy spectrum. However, the sensor's collection of this information does not guarantee an improvement in the performance of the user. This is because the information is still subject to the capabilities and limitations of the sensor, CRT display and the user himself.

The purpose of this paper is to analyze some of the limitations of the CRT display, more precisely, those limitations which are a result of the interaction of the CRT's phosphor and the information refresh rate. The criterion of importance is the capability of the display phosphor to accurately present amplitude and phase information for static and dynamic targets. Recent emphasis on low level and nap-of-the-earth (NOE) flights has increased the interest in the capability of CRT displays to accurately present dynamic targets.

FUNDAMENTALS OF CRT DISPLAY SYSTEMS

INTRODUCTION

The function of a CRT system is to produce a faithful reconstruction of a scene which is under the sensor's surveillance. This function is straightforward in theory, but complicated in implementation. For this reason, it is necessary to provide some basic background on the underlying principles and mechanisms involved in the image production. This understanding will better prepare the reader to follow the derivations of the limitations of the display in its attempt to produce a "satisfactory" image.

The simplified block diagram in Figure 1 illustrates an electro-optical imaging system utilizing a CRT display. A sensor produces an electrical analog of a scene and transmits this electrical signal to a display, where it is transduced back into light output for viewing and interpretation by the user.

SCENE   SENSOR → CRT DISPLAY → USER
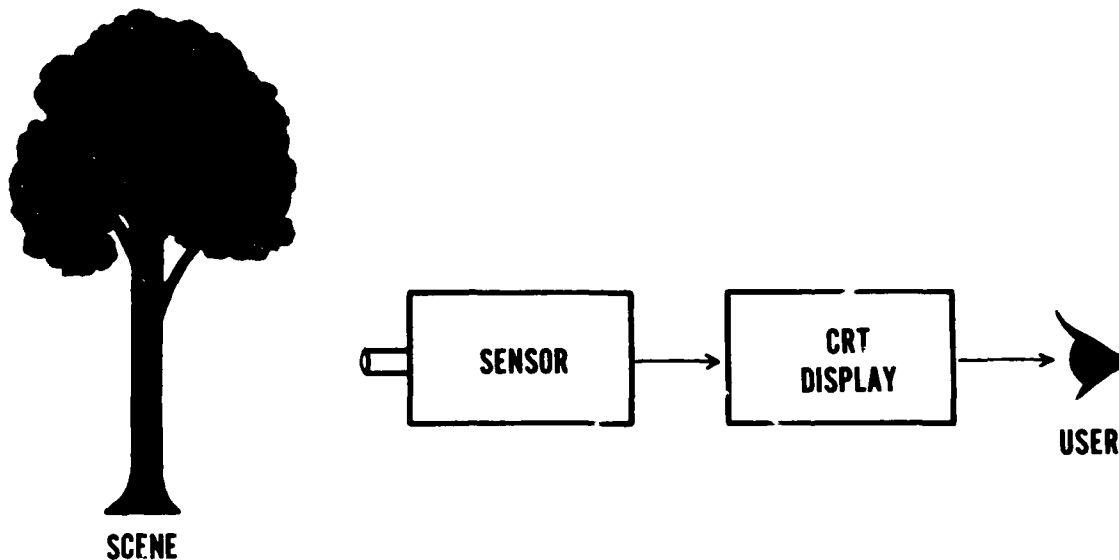
FIGURE 1. Block diagram of an electro-optical imaging system.

IMAGE RECONSTRUCTION

Even though this investigation is concerned with the image degradation resulting from the CRT display only, it is beneficial to discuss the method of image production beginning with the sensor. Figure 2 shows an electro-optical sensor which utilizes a line-scan technique typical of CRT systems. A scene is focused onto a photoconductive sensor, the surface of which varies its electrical conductance in proportion to the amount of light falling upon it. In this manner the luminance profile of the scene is converted into a conductance profile on the sensor. An electron gun then scans the conductance profile with an electron beam. A set scan pattern is used, resulting in a temporal voltage signal representative of the conductive profile and, therefore, the luminance profile of the scene.

The scan pattern of the electron beam is controlled by a beam deflection system which moves the beam in horizontal lines across the image resulting in a set of output signals which are representative of the image from top to bottom. At the end of each horizontal line-scan, the beam is returned to the start of the next line by an action known as the horizontal retrace. At the end of the full set of horizontal line-scans, the beam is returned to the top of the image by means of a vertical retrace. Figure 3 shows the path of the
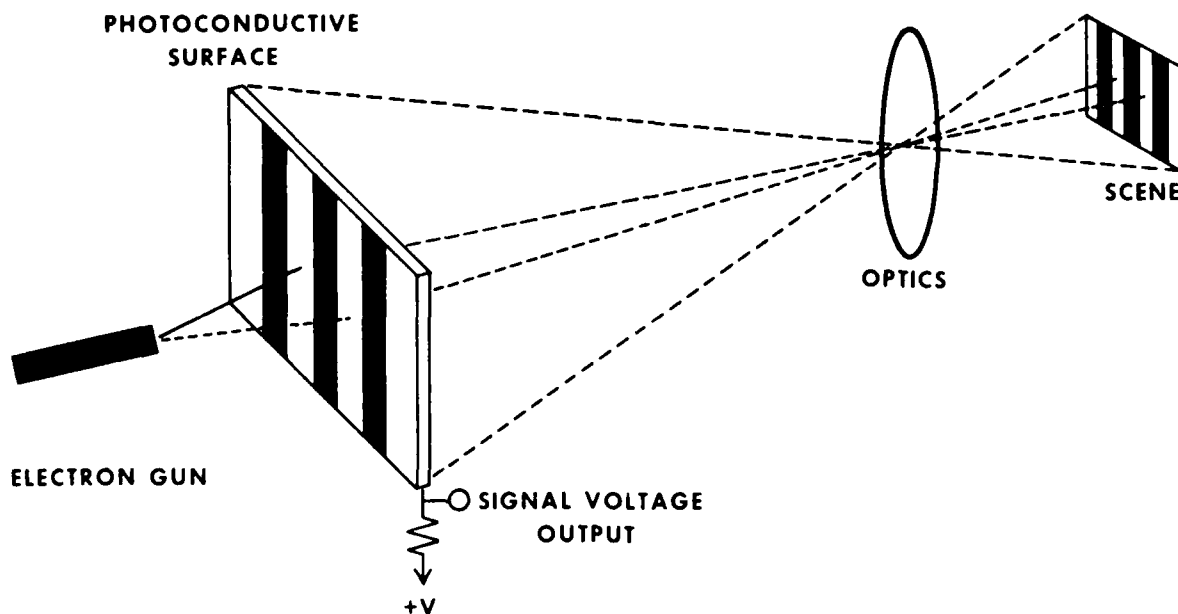
FIGURE 2. Line-scan imaging system.

beam during the scanning procedure. Using this procedure, the scan of a bar pattern (Figure 4A) will produce a temporal voltage signal like that shown in Figure 4B. Only two line-scans are depicted here, but the total voltage representation of the image would consist of the entire set of horizontal line scans. Many commercial line-scan imaging systems use a total of 525 scan lines to reproduce an image. The full reproduction of an image is called a frame, and the number of times per second that the full image is scanned is called the frame rate of the imaging system. One frequently encountered frame rate is 30 frames/sec. This means that the image is scanned and electrically reproduced every 1/30 of a second. However, if a new picture is presented to the eye at the rate of 30 pictures/sec, the image will appear to flicker. This is overcome by means of a technique known as interlacing.

In interlacing, a frame is actually scanned in two parts known as "fields." Referring again to Figure 3, if only the odd lines (n=1,3,5,...) were scanned first, followed by a vertical retrace, and afterward only the even lines (n=2,4,6,...) were scanned, then the image or frame would be represented by two fields. For a frame rate of 30 frames/sec, we have a field rate of 60 fields/sec. The ability to reproduce an image in this way lies in the persistence characteristics of the display phosphor. (Note: A full discussion of phosphors is provided in a later section.)

9
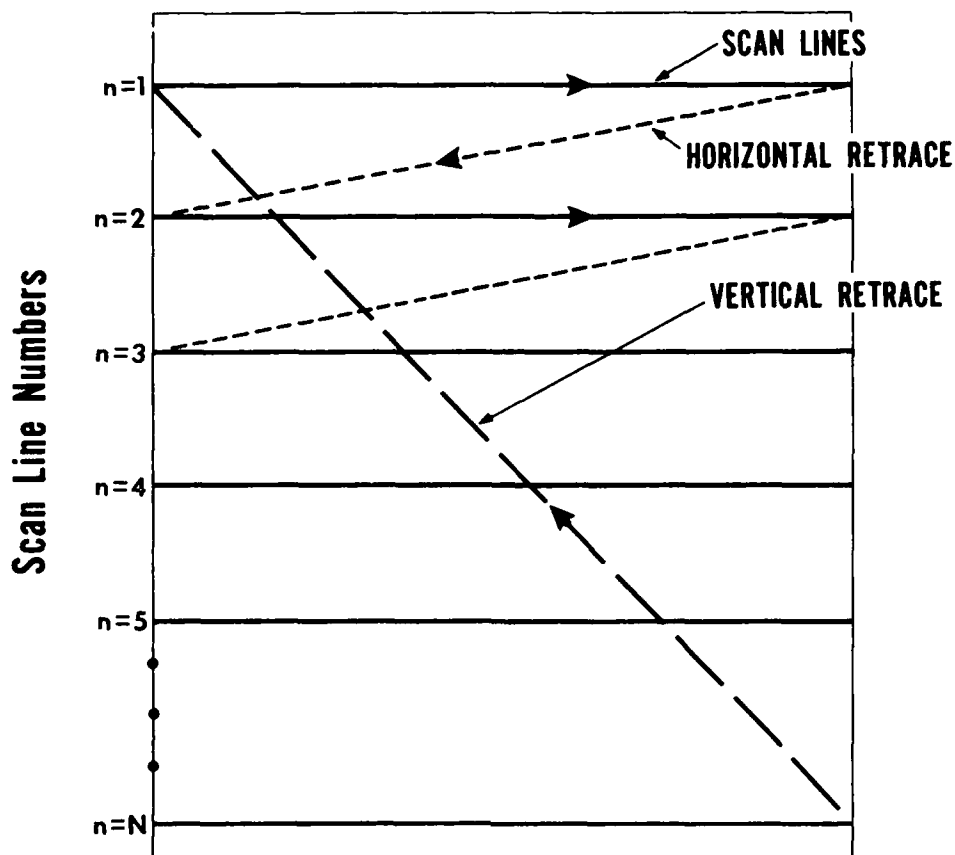
FIGURE 3. Line-scan path.

So far the description of the CRT system has been confined to the sensor (or camera). The display, which makes up the second half of the imaging system (refer to Figure 1) is more important in this discussion, for we are investigating its limitations. The CRT display is the part of the system in which the voltage representation of the scene produced by the sensor is transformed back into a luminance profile. This transformation is accomplished by causing a second electron beam, synchronized with the scanning beam in the sensor, to produce on a display screen a luminance profile which varies in intensity along a line across the screen in proportion to the input signal voltage.

The synchronization of the two scanning beams is accomplished by means of horizontal and vertical sync pulses created at the sensor electronics and transmitted to the display along with the signal voltage. In the display electronics, the sync pulses are removed from the input signal and are used to control the synchronization of horizontal and vertical oscillators in the deflection circuitry.
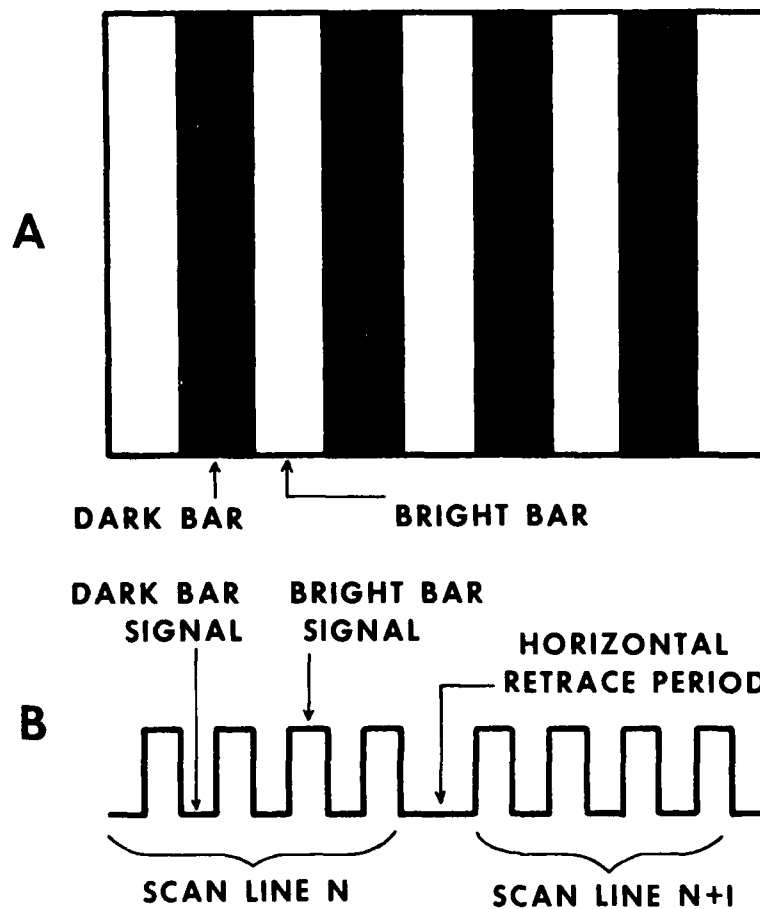
FIGURE 4. (A) Typical bar pattern and (B) its temporal voltage representation.

The CRT consists basically of an electron gun and phosphor screen in an evacuated glass envelope (See Figure 5). Located between the electron gun and the phosphor screen is the deflection system. The two types of deflection systems are electrostatic and magnetic. In the case of electrostatic deflection, depicted in Figure 5, two pairs of deflection plates, a pair of vertical plates and a pair of horizontal plates, are used to position the electron beam. For magnetic deflection, a coil is placed around the outside of the glass envelope.

These two deflection systems differ in sensitivity to acceleration voltage. The electrostatic method is subject to beam distortion and is used only in tubes requiring low deflection angles. The more universally utilized magnetic deflection method provides for higher resolution and brightness, desirable image qualities.

11
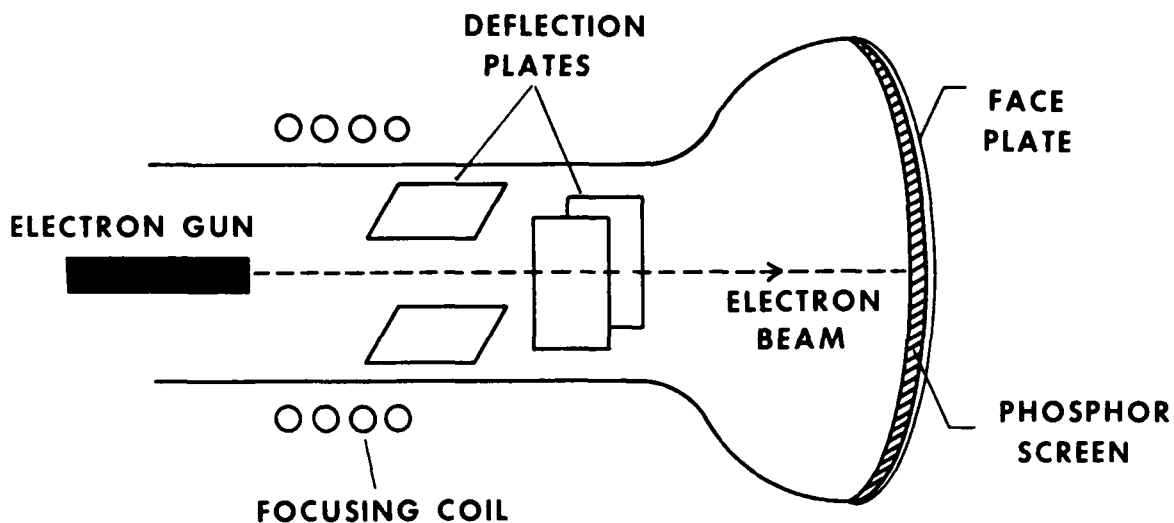
FIGURE 5. Typical parts of a cathode-ray-tube (CRT).

One final manipulation of the electron beam is required. As the electron beam travels out from the electron gun, it tends to spread. A spreading of the electron beam as it traverses the tube would result in a very low resolution picture. This is overcome by focusing the electron beam upon the phosphor screen. The two methods of focusing are again magnetic and electrostatic. As with deflection, each focusing method has its advantages and disadvantages (Westinghouse, 1981). The electrostatic method is the more widely used due to its high resolution capabilities.

PHOSPHORS AND THEIR CHARACTERISTICS

The word "phosphor" is generally used in CRT terminology to designate a substance that emits light when struck by electrons (Leverenz, 1950). This production of light by electron bombardment is called cathodoluminescence. In this process, the incident electrons free others within the phosphor (Levi, 1968). Together these electrons excite luminescence centers. The region of excitation tends to assume a spherical shape. The size of the sphere increases with increasing electron energy. At extremely high excitation energies, the region eventually becomes a cylindrical channel. (See Figure 6.)

The process of cathodoluminescence occurs in two stages, fluorescence and phosphorescence. These two stages are distinct because of the timing of the emission of the radiation with respect to the excitation. Fluorescence is
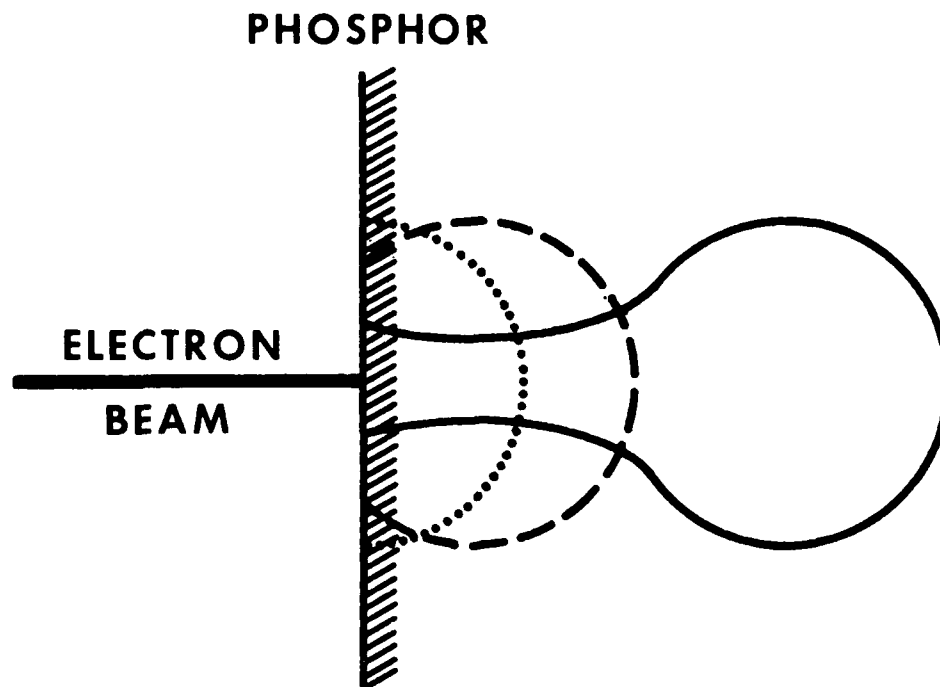
PHOSPHOR

FIGURE 6. Region of excitation showing increasing electron energy (Farrell and Booth, 1975).

emission immediately following the excitation. Phosphorescence implies an appreciable delay between the emission and the excitation. Fluorescence occurs only during the period that the electrons are striking the phosphor and ends within about 0.01 microseconds after the end of the bombardment (Farrell and Booth, 1975). Phosphorescence may persist over periods extending from a fraction of a microsecond to hours.

Figure 7A shows typical growth and decay curves for a cathodoluminescent phosphor. The initial growth can be rapid and is due to fluorescence only. If the electron excitation continues, the resulting intensity is a combination of fluorescence and phosphorescence. When the excitation is removed, the fluorescence decays very rapidly while the phosphorescence decays over a much longer period.

Figure 7B illustrates more precisely the type of luminescence buildup which will occur in a CRT display where the rate of excitation is much higher than the decay rate. A maximum intensity is obtained when the phosphor becomes saturated. At this point no further increase in light production is possible, not even with further increases in electron density. This condition of saturation is not a desired effect in most situations.

13
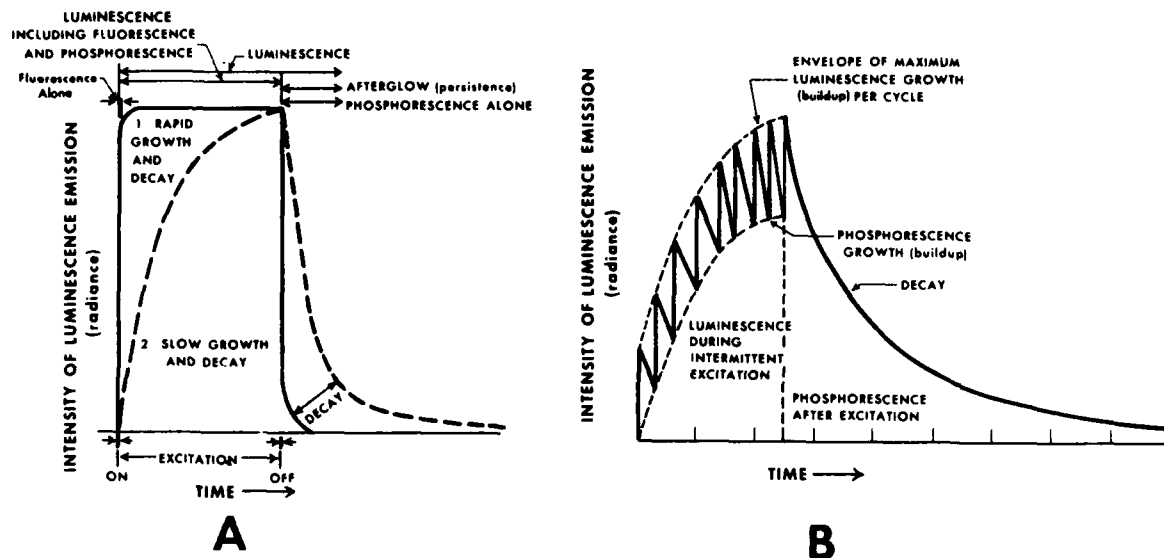
FIGURE 7. (A) Typical growth and decay curve, and (B) luminescence buildup (Leverenz, 1950).

The phosphor characteristics introduced above are more generally defined using the terms "rise time" and "decay time," the latter also being called "persistence." Rise time is generally accepted as the time taken for the intensity to increase to 90% of the peak luminance. Peak luminance is the maximum brightness attained for a given set of excitation conditions. Persistence is defined as the time required for the intensity to decay to 10% of its peak value.

Phosphors are classified by their persistence. Those requiring less than 1 microsecond to decay to 10% of their peak luminance are classified as very short phosphors. Table 1 gives a full listing of the phosphor classes. The persistence can be determined experimentally by measuring the phosphor's response to a single pulse excitation or by determining its temporal modulation transfer function (Shires, 1979). Typical phosphors used in industry with persistence characteristics as short (P24), medium (P43) and long (P12) are given in Figure 8.

In addition to rise time and persistence, other phosphor characteristics include color, efficiency, and usable lifetime. Color, perhaps, is the most important visual phosphor characteristic and, fortunately, is generally independent of operating conditions. All phosphors emit radiation over a band of wavelengths. However, each generally has one peak wavelength about which a narrow band accounts for most of the energy output. Figure 9 shows the spectral energy emission characteristics for P1, P5, and P43 phosphors. P1 has a

14

TABLE 1

PHOSPHOR CLASSES BY PERSISTENCE*

Persistence	Class
> 1 sec	Very long
100 msec to 1 sec	Long
1 to 100 msec	Medium
10 μsec to 1msec	Medium short
1 to 10 μsec	Short
< 1 μsec	Very short

* Westinghouse Electric Corp, 1972.

SHORT
P24
DATA FROM MAY
1955 REGISTRATION

MEDIUM
P43
ANODE VOLTAGE=15 KV
ANODE CURRENT=5 μa

LONG
P12
ANODE VOLTAGE 3.0 KV
ANODE CURRENT 1.5 μa

Relative Brightness Percent of Maximum

MICROSECONDS   MILLISECONDS   MILLISECONDS
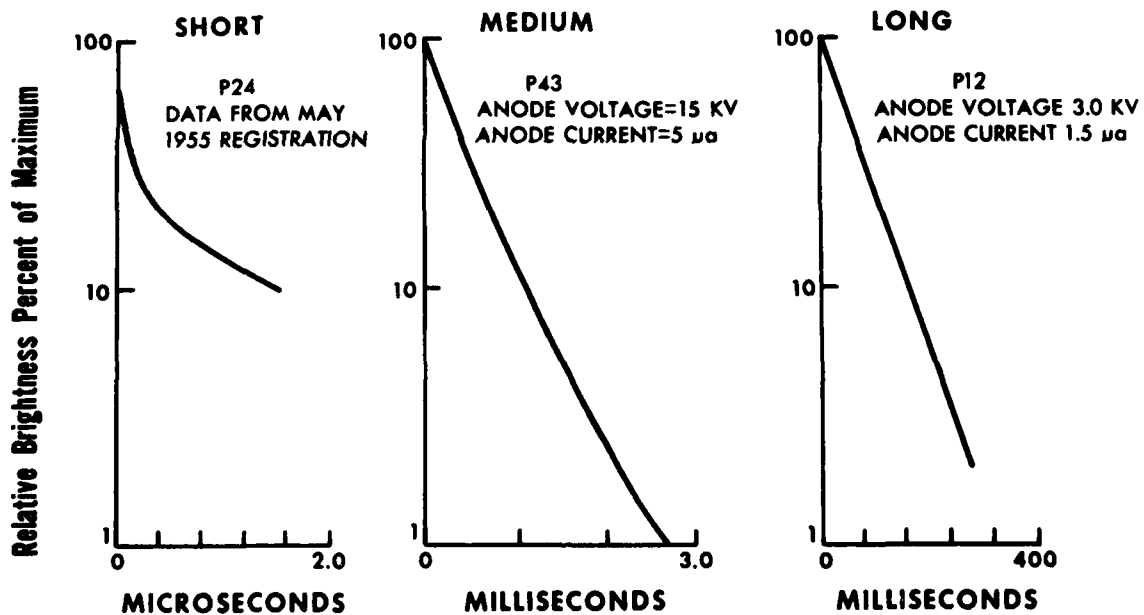
FIGURE 8. Persistence characteristics for a short (P24), medium (P43), and long (P12) phosphor. (Westinghouse Electric Corporation, 1972)

15

yellowish-green color; P5 is blue; P43 is also yellowish-green. The colors of many other phosphors as well as a listing of other characteristics of most industrial and military phosphors can be found in Table 2.

The efficiency of a phosphor, as used here, will be defined as luminous efficiency, i.e., lumens per watt, which defines efficiency in terms of the human eye response. Many factors are involved in producing a phosphor of desired efficiency, e.g., type of activators, temperature, batch preparation, and raw material purification. Efficiency variations of 10% are typical between separate, yet identical preparations.
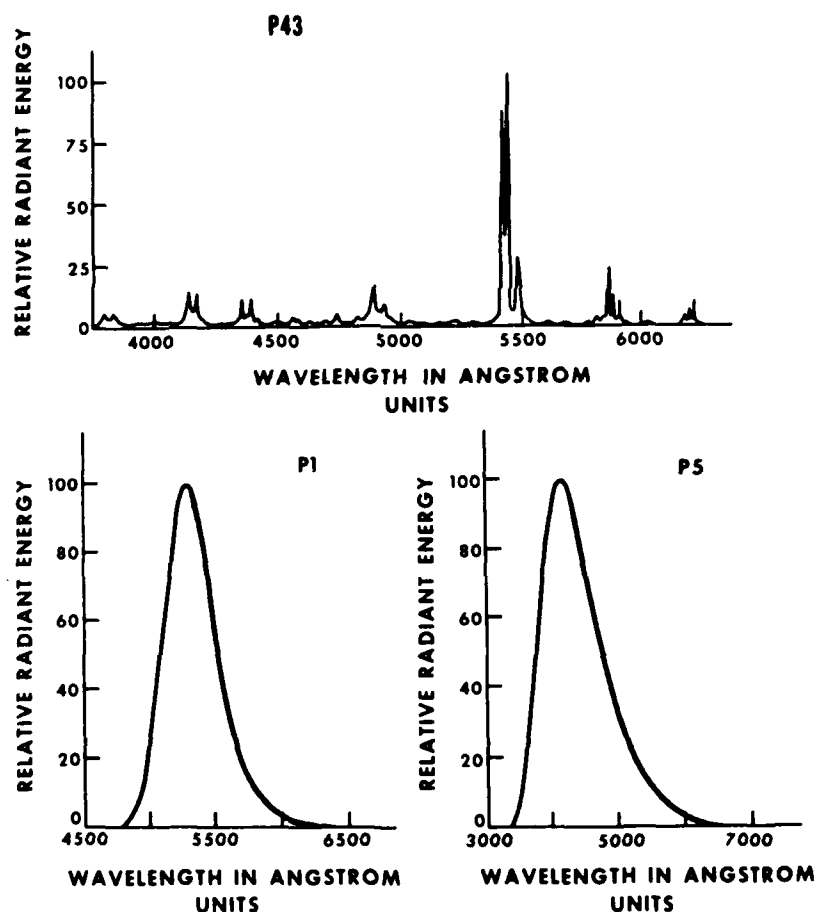
FIGURE 9. Spectral energy emission characteristics of P43, P1, and P5 phosphors. (Westinghouse Electric Corp., 1972)

16

TABLE 2

CHARACTERISTICS OF STANDARD PHOSPHORS*

PHOSPHOR NUMBER	PHOSPHORESCENT COLOR	RANGE NANOMETERS	PEAK (S) NANOMETERS	CLASS	PERSISTENCE (10%)
1	Yellowish-Green	492 to 577	525	Medium	24 mSec.
2	Yellowish-Green	435 to 612	535	Medium Short	36 uSec.
4	White	Note 1	Note 1	Medium Short	60 uSec.
5	Blue	352 to 560	415	Medium Short	16 uSec.
7	Yellowish-Green	400 to 650	440 & 555	Long	0.3 Sec.
11	Blue	400 to 550	460	Medium Short	80 uSec.
12	Orange	540 to 680	590	Long	0.21 Sec.
13	Red	580 to 800	640	Medium	50 mSec.
14	Yellowish-Orange	390 to 710	440 & 600	Medium	5 mSec.
16	Bluish-Purple	350 to 450	385	Very Short	0.5 uSec.
19	Orange	550 to 672	590	Long	0.22 Sec.
20	Yellow-Green	495 to 672	560	Medium Short	0.35 mSec.
22	Note 3	412 to 702	3 Peaks	Note 2	Note 2
24	Green	432 to 630	510	Short	1.5 uSec.
25	Orange	532 to 715	610	Medium	45 mSec.
26	Orange	545 to 665	595	Very Long	1.8 Sec.
27	Reddish-Orange	582 to 715	631	Medium	27 mSec.
28	Yellow-Green	465 to 632	548	Long	70 mSec.
31	Green	417 to 597	522	Medium Short	30 uSec.
32	Yellowish-Green	385 to 655	554	Long	0.7 Sec.
33	Orange	545 to ---	587	Very Long	0.38 Sec.
34	Yellow-Green	390 to 680	529	Very Long	100 Sec.
36	Yellowish-Green	475 to 670	550	Very Short	0.25 uSec.
37	Blue	390 to 560	470	Very Short	0.16 uSec.
38	Orange	530 to 680	600	Very Long	1.05 Sec.
39	Yellowish-Green	488 to 580	525	Long	150 mSec.
40	Yellowish-Green	650	435 to 560	Long	0.55 Sec.
	Greenish	540 to 660	590	Long	0.2 Sec.
41	Yellow			Very Short	U V 0.12 uSec.
42	Yellowish-Green	451 to 592	520	Medium	8 mSec.
43	Yellowish-Green	540 to 560	542 to 545	Medium	1.2 mSec.
44	Yellowish-Green	540 to 554	542 to 545-547	Medium	1.2 mSec.
45	White	--- ---	545 Many Peaks	Medium	1.8 mSec.

* Westinghouse Electric Corp., 1972.

Note 1. P4 is available in various mixtures.
Note 2. Persistence varies per component.
Note 3. Tri-color pattern resulting in white appearance.

The last phosphor characteristic to be discussed is usable lifetime. As the phosphor accumulates excitation time, its luminescent efficiency decreases (Levi, 1968). This decrease is generally continuous and asymptotically approaches some final value that is only a small fraction of the initial value. No definite law of deterioration has been developed since operating conditions and preconditioning greatly affect the long-term performance (Larach, 1965). Life times (to half-brightness) can range between 1000 and 10,000 hours.

IMAGE QUALITY

The factors which affect the quality of a CRT image can be both subjective and objective. In Task's (1979) investigation of display system "figures of merit" (FOMs) which can be used to indicate image quality in CRT displays, he subdivided CRT display system parameters into three categories: geometric, electronic, and photometric. Table 3 shows the distribution of the various parameters into these three categories.

TABLE 3

TELEVISION DISPLAY SYSTEM PARAMETERS*

Geometric	Electronic	Photometric
Viewing Distance	Bandwidth	Luminance
Display Size	Dynamic Range	Gray Shades
Aspect Ratio	Signal/Noise	Contrast Ratio
Number of Scan Lines	Frame Rate	Halation
Interlace Ratio	Field Rate	Ambient Illuminance
Scan Line Spacing		Color
Linearity		Resolution
		Spot Size and Shape
		Modulation Transfer Function
		Luminance Uniformity
		Gamma

* Task, 1979.

Even a brief discussion of each of these parameters would require more space than can be allocated in this paper. Discussion will therefore be limited to those parameters which bear more directly on the subject of image quality. These parameters include luminance (brightness), contrast, frame rate, field rate, resolution, spot size and shape, and modulation transfer function (MTF).

Brightness

Recommending an optimum brightness for an image is difficult. Typical peak brightness values range from 30 to 100 footlamberts with a minimum of 10 footlamberts recommended under even the best viewing conditions (Goldmark, 1949), e.g., low ambient lighting, no glare sources, and high contrast.

Contrast

The use of the term "contrast" in CRT work refers to the ratio of the maximum to the minimum luminance on the screen. Contrast ratios of 50:1 to 100:1 are typically adequate for effortless viewing (Goldmark, 1949). The greater the contrast ratio of a CRT, the greater the number of quantized levels possible. These levels of luminance steps are referred to as "gray-scale" steps, generally accepted as equal logarithmic steps which increase by a factor equal to $\sqrt{2}$ between each step. The number of gray-scales possible introduces a concept known as the "dynamic range" of the system. For example, a system having 14 gray-scales would possess a dynamic range of $(\sqrt{2})^{14} = 128$. The contrast capability of the system can be measured by the number of gray steps that can be reproduced.

Frame Rate and Field Rate

The frame rate of a CRT system is the frequency at which the video picture is fully updated, whereas the field rate is the frequency at which a full picture is written on the screen. The continuity of the picture is dependent on the field rate which must be high enough to represent motion in an "apparently" continuous manner while avoiding the presence of flicker.

A field rate of 60 per sec is considered to be sufficient to fuse discrete movements of an object, providing the object does not move across the frame at too excessive a rate. It can be pointed out here, however, that a selected field rate does imply a maximum object/sensor relative velocity above which motion may be marked by visible jerks in the progress of the object across the screen.

19

Resolution

Spatial resolution is perhaps one of the most important parameters in determining the picture quality of an imaging system. As the size of the picture elements decreases, the sharpness of the picture increases to some limiting value determined by pixel size (Seyrafi, 1973). The ability of an imaging system to represent the fine detail in a scene is referred to as the resolution of the system. In television the resolution is measured by the maximum number of adjacent parallel lines which may be produced in the image. The term "TV lines of resolution" generally refers to the maximum number of horizontal lines which can be accommodated within the vertical height of the display. This is, of course, dependent on the number of scan lines being used in the imaging sensor. Current industry standards provide about 490 scan lines. For reasons which are not relevant here, this number is reduced to approximately 350 vertical resolution lines (Farrell and Booth, 1975).

Next we consider the horizontal resolution. We will start with the simple statement that a measure of horizontal resolution is the maximum number of parallel vertical bars which can be accommodated within the width of the display. More precisely, we can say that since the lines (or bars) represent changes in voltage applied to the electron gun during a horizontal scan, the horizontal resolution can be measured by the maximum number of voltage changes which can occur during a single line scan. The frequency with which this maximum number of voltage variations occurs is called the "bandwidth." Figure 10 shows a bar pattern and the relationship between the voltage variations and the picture elements (pixels).
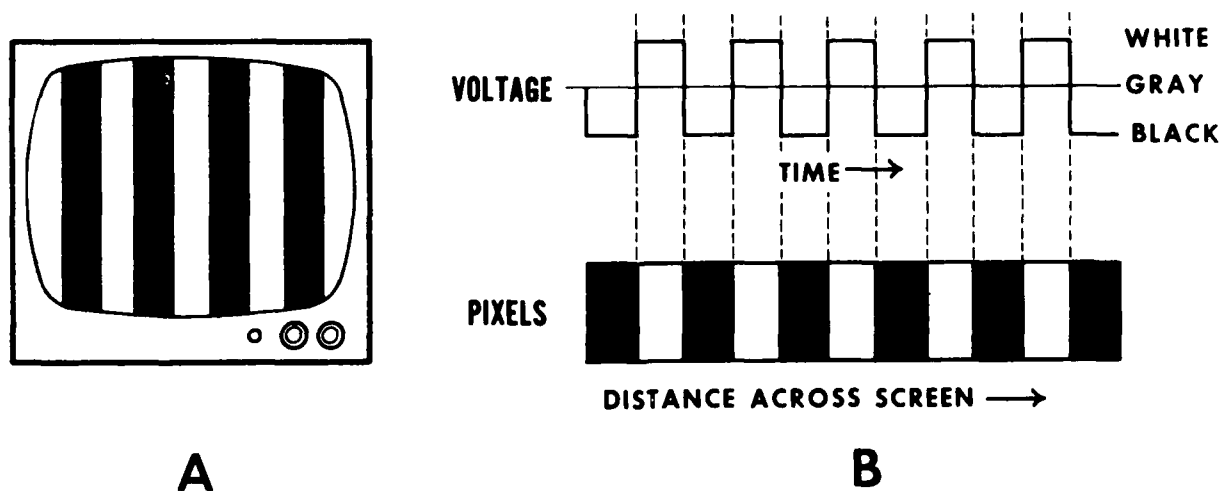
FIGURE 10. (A) Bar pattern on display face and (B) relationship between voltage variations and picture element.

20

The horizontal resolution as noted above can be stated as the maximum number of vertical lines (or bars) which can be produced on the display. Since each black and white (dark and bright) line or bar pair can be regarded as a full cycle of the signal voltage, the term "spatial frequency" is often used to represent the number of bright and dark pairs of bars present on a display (see Figure 11). The spatial frequency can be expressed in terms of cycles per display width or cycles per unit distance across the display (e.g., cycles/mm or cycles/inch). A typical maximum value of spatial frequency for CRT displays is 400 cycles/display width.

BRIGHT BARS
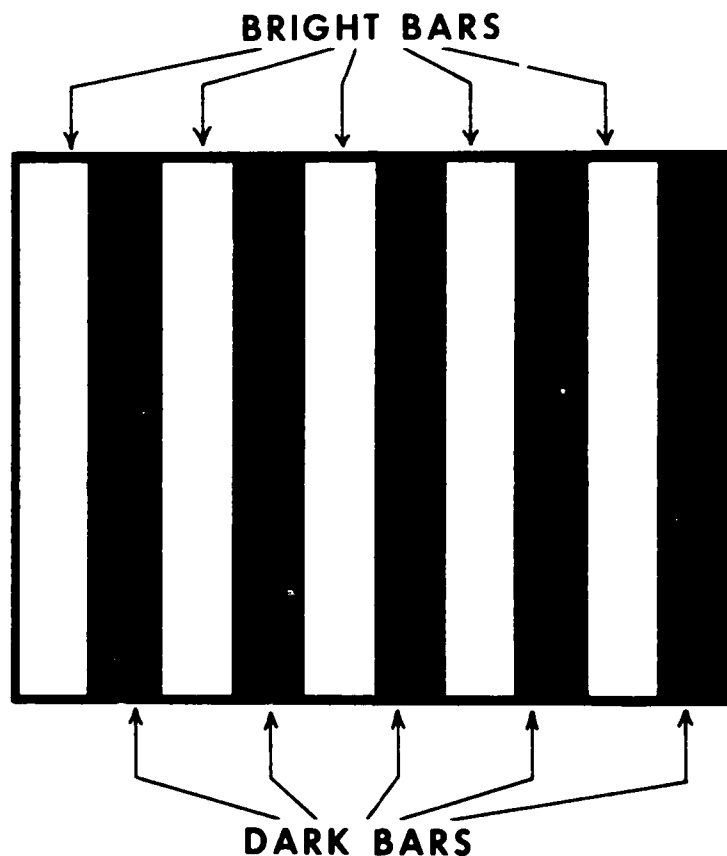
DARK BARS

5 DARK BARS
5 BRIGHT BARS

TOTAL = 10 BARS
SPATIAL FREQUENCY = 5 CYCLES
PER DISPLAY

FIGURE 11.   Definition of spatial frequency.

Spot Size and Shape

Related somewhat to resolution is the size and shape of the spot formed on the phosphor screen by the electron beam. In analyzing the anatomy of the CRT spot, both the current distribution in the electron beam and the spreading of the light on the phosphor screen are points of consideration (Levi, 1968). The current is highest in the center of the spot and decreases in the manner shown in Figure 12. This distribution is a Gaussian curve and is plotted as a function of distance in standard deviations (σ) out from the center of the spot. Since in a Gaussian distribution the current never decreases to zero, it is customary to choose some point on the curve to serve as an arbitrary measure of the spot's diameter. One commonly chosen value is the 50% point on the curve.

FIGURE 12. Spot size and shape (Zworykin and Morton, 1940).

22

The lack of a finite diameter for the light distribution of a spot on the phosphor screen raises a question concerning the obvious overlapping of Gaussian scan lines. The luminance value at a single point, even without consideration of scattered or ambient light, is the mathematical summation of the contributions of every scan line above and below it. A full treatment of this topic can be found in Jenness, Eliot, and Ake (1967).
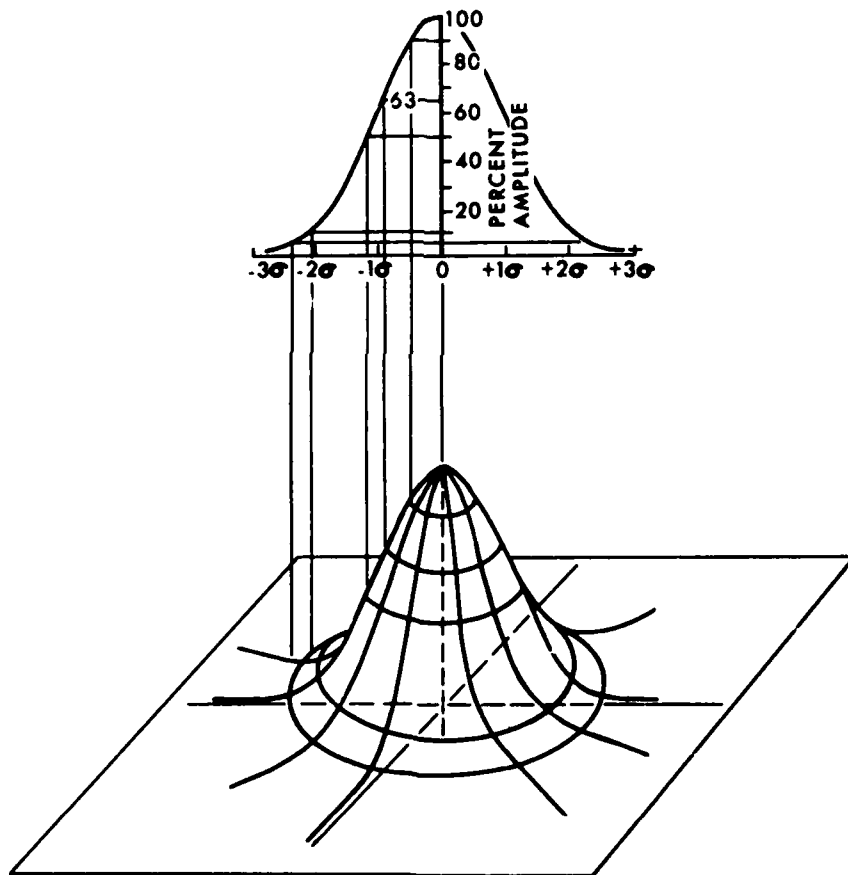
The term "spot size" in the above discussion has been used to convey two distinct, but related, descriptions of the CRT spot. One refers to the geometric shape of the spot; the other refers to the distribution of the light within the spot. The latter is more properly referred to as the point spread function (Farrell and Booth, 1975). So, more precisely, the CRT spot can be described as circular in shape with a Gaussian point spread function.

Modulation Transfer Function

The last measure of CRT image quality to be presented is the one which is currently most used. It is the modulation transfer function (MTF). For displays where the information to be presented is either rapidly changing or is of high density, it is advantageous and necessary to know how accurately the CRT responds to the modulation of the electron beam. As applied to CRTs, the MTF measures the sine wave frequency response of the CRT system from electronic input to visual output (Spearnock, 1979). In more precise terms, the MTF of the display system indicates the system's capability to transfer contrast from the input scene to the output image as a function of spatial frequency. The MTF can experimentally be obtained by first modulating the electron beam with a specific frequency sinusoidal signal. The resulting sinusoidal spatial luminance pattern on the phosphor screen is then scanned by a photometer and the amplitude of the luminance pattern recorded. The modulating signal is progressively increased in frequency, repeating the measurements. The obtained amplitude values are normalized to the low frequency values. (Note: the transfer factor is assumed to have a value of 1 at very low frequencies.) A plot of the normalized values as a function of spatial frequency is the MTF. A typical MTF curve is shown in Figure 13. A detailed methodology for obtaining the luminance profile on the face of a CRT can be found in Virsu and Lehtiö (1975).

For an MTF to validly describe a system, the response of the system must be uniform throughout the field of view (homogeneous) and in all directions (isotropic) and the response must be independent of input levels, i.e., possessing the properties of a linear system (Cornsweet, 1970). CRT systems approximate all of these properties except one; the CRT system is anisotropic (Keesee, 1976). The imagery presented on the CRT is the result of continuous sampling in the horizontal direction but discrete sampling in the vertical direction. This departure from a linear system strictly means that two MTFs (one vertical and one horizontal) are required. However, the horizontal MTF is the more commonly utilized FOM.
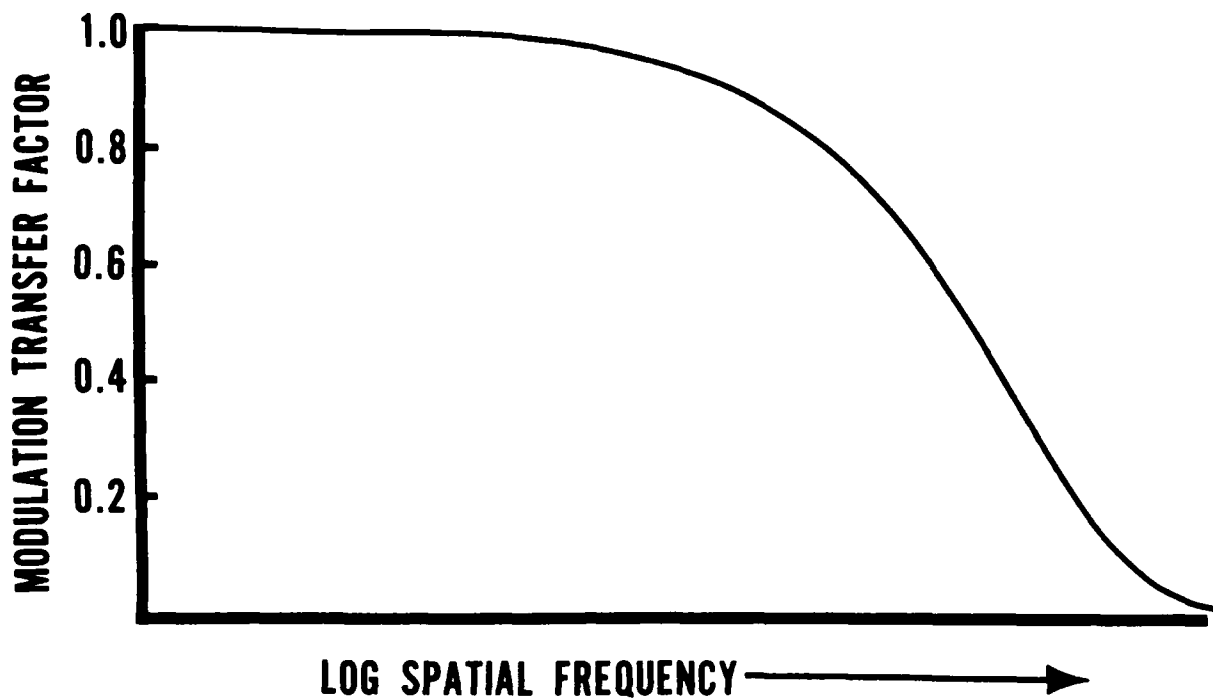
FIGURE 13. Typical Modulation Transfer Function curve.

IMAGE DEGRADATION

This section will provide a brief introduction to the types of image defects inherent in CRT display systems. These include flicker, ripple, and interlace pairing.

Flicker is defined as a visual sensation produced by periodic fluctuations in light at a rate less than a few cycles per second. It has long been known that the human eye does not generally perceive discontinuity in a motion at frequencies above approximately 15 cps. Motion pictures make use of this characteristic by projecting pictures of a changing scene at a rate high enough to achieve an illusion of continuous motion. This illusion is possible due to the eye's "persistence of vision." Above a "critical fusion frequency," dependent on luminance, color, duty cycle, and retinal position of the source, the eye fuses the light variation into a steady perception (Cornsweet, 1970). CRT's attempt to eliminate or reduce flicker by operating at a field rate that is above the critical fusion frequency dictated by the operating range of the display.

When a Gaussian spot sweeps over a phosphor screen at a constant velocity, it generates a scan strip across which the phosphor brightness is also Gaussian (Jenness, et al, 1967). The mathematical derivation of this fact points out

24

the presence of a ripple in the resulting vertical brightness profile. This ripple appears as an unwanted modulation on the display. The amount of ripple present will affect the maximum contrast with which the display can produce a test pattern of minimum-width stripes parallel to the scans.

As mentioned in an earlier section, a CRT system normally generates a picture frame produced by two interlaced fields. The odd numbered lines are scanned in one field and the even numbered lines are scanned in a second field. Ideally, the even numbered lines fall exactly halfway between the odd numbered lines (Figure 3). If such is the case, the CRT system is said to be "perfectly interlaced." If the odd and even numbered lines do not fall exactly between each other, the system is said to be paired. A completely paired system, one in which the even and odd lines are superimposed, has effectively only half as many scan lines as it should. This results in only half the resolution capability. Various lesser degrees of interlace pairing will result in corresponding degrees of loss in detail response. A full discussion of this type of resolution degradation and methods of measuring it can be found in Hurford's (1967) article.

MATHEMATICAL DESCRIPTION OF CRT DISPLAYS

SCANNING THEORY

The mathematical derivation of scanning theory is quite complicated. Therefore, this discussion will make use of intermediate results first presented by Mertz and Gray in 1934. A more recent presentation can be found in Levi (1968).

Levi (1968) presents the CRT system as a case of discrete imaging. Actually, a raster scan system is continuous in one direction and discrete in the transverse direction. A one-dimensional sampling system (the raster scan) maps a two-dimensional object into a one-dimensional image, an electrical signal.

The scanning electron beam on the photoconductive surface acts as a scanning aperture with transmittance distribution g_0 (x,y), traversing the image of the object with a horizontal speed v in a set of scan or raster vertical lines Δy apart. The signal produced by examining the scene $s(y)$ can be written as

$$s'(x;j) = \iint s(x',y')g_0(x'-x,y'-j\Delta y) \, dx'dy',$$ Eq. 1

where x is the origin position of the scanning aperture in the object plane coordinate, j is the raster line number referenced to the origin of the object coordinate system, and x' and y' represent the aperture coordinate system.

The required transformation into the time coordinate is made using the relationships

$$x = vt^* \text{ and} \qquad \text{Eq. 2}$$

$$j = \left[\frac{t}{\Delta t}\right], \qquad \text{Eq. 3}$$

where Δt is the period of a single line scan including retrace, v is the scanning speed, and the brackets indicate only the integer portion of the result. The time t^* is defined as

$$t^* = t - \Delta t \left[\frac{t}{\Delta t}\right] \qquad \text{Eq. 4}$$

and represents the time elapsed since the beginning of a distinct line scan. The resulting expression of the signal is

$$s'(t) = \iint s(x',y')g_0(x'-vt+v\Delta t\left[\frac{t}{\Delta t}\right], y'-\left[\frac{t}{\Delta t}\right]\Delta y)dx'dy'. \qquad \text{Eq. 5}$$

The signal $s'(t)$ will be operated upon by signal processing electronics having a response of $g_t(t)$, resulting in a third representation of the object expressed as

$$s''(t) = s'(t) \circledast g_t(t) \qquad \text{Eq. 6}$$

When $s''(t)$ is combined with a synchronized display raster scan (velocity, v', and vertical line spacing, $\Delta y'$), a luminance pattern is reconstructed in the image plane. Levi (1968) gives the resultant intensity at any point (x'',y'') in the image plane as

$$s'''(x'',y'') = \sum_j \int_{j\Delta t}^{(j+1)\Delta t} s''(t)g_1(x''-t^*v',y''-j\Delta y')dt \qquad \text{Eq. 7}$$

where $j\Delta t, (j+1)\Delta t$ represents the start and end times for the scan, respectively, t^*v' represents the x-coordinate of the position of the scanning spot origin at time t, and $g_1(x,y)$ represents the spread function of the image scan spot.

In a CRT the image spot is formed on a phosphor screen, a medium, which for display purposes, has a finite memory. For this reason the term g_0 introduced in Equation 1 must incorporate the concept that the instantaneous spot luminance value is dependent on the luminance history of the phosphor pixel. This dependency is the subject of later discussion.

FLAT FIELD

Perhaps the simplest target to "look at" with a sensor is one of uniform luminance, one which is both isoplanatic and time invariant. Such a target, when scanned, would result in a modulation of zero on the reconstructing display electron beam. This will produce an image which, neglecting noise, would be equally isoplanatic and time invariant, at least as measured by a photometer which has an integration time several times greater than the field rate of the display. However, if we consider times shorter than the field rate periods, and the display to be composed of small areas (pixels) equal to or smaller than the electron beam spot size, then, as we have seen from the previous discussion of phosphors, the intensity of the phosphor in the region being investigated varies over time. The intensity of the pixel will rise rapidly during excitation and then decay towards zero until re-excited. If a very fast photometer (short integration time, less than the vertical field period) is mapped onto a pixel, then the photometer output as a function of time will be similar to that shown in Figure 14. From this picture of the intensity of a single pixel, as a function of time, the interaction between the display field rate and the phosphor's persistence calls attention to itself. For short persistence phosphors the pixel's intensity will decay appreciably before re-excitation occurs. But, with long persistence phosphors, the re-excitation occurs before the pixel can decay appreciably. (See Figure 15)

If we assume the decay to be exponential, as a first order approximation, then the intensity of a single pixel after a single excitation can be expressed as

$$I(t) = I_0 e^{-\alpha t} \hspace{4cm} \text{Eq. 8}$$

where t is measured from the end of the excitation, and α is related to the 10% persistence, τ, by the following expression,

$$\alpha = 2.3/\tau \hspace{4cm} \text{Eq. 9}$$

So, Equation 8 can be re-expressed as

$$I(t) = I_0 \exp(-2.3t/\tau) \hspace{3cm} \text{Eq. 10}$$

We will make note of the fact that a pixel will require a period of 2τ to decay to 1% of its maximum intensity. A decay period of 5τ will be chosen to represent a time after which the intensity is essentially zero.

As mentioned earlier, a particular pixel in a raster scan display is re-excited at the vertical frame rate frequency. Current standards use a frame rate of 30 Hz, therefore each pixel is re-excited every 33.33 msec. This means that unless the phosphor pixel under investigation has a phosphor persistence (10%) of less than 6.66 msec (1/5 of 33.33 msec), the pixel has residual luminance from the nth excitation when it is excited for the $(n+1)^{th}$ time. Actually, the pixel's intensity at some time t is a summation of the residuals of all past excitations until saturation is reached. In other words,
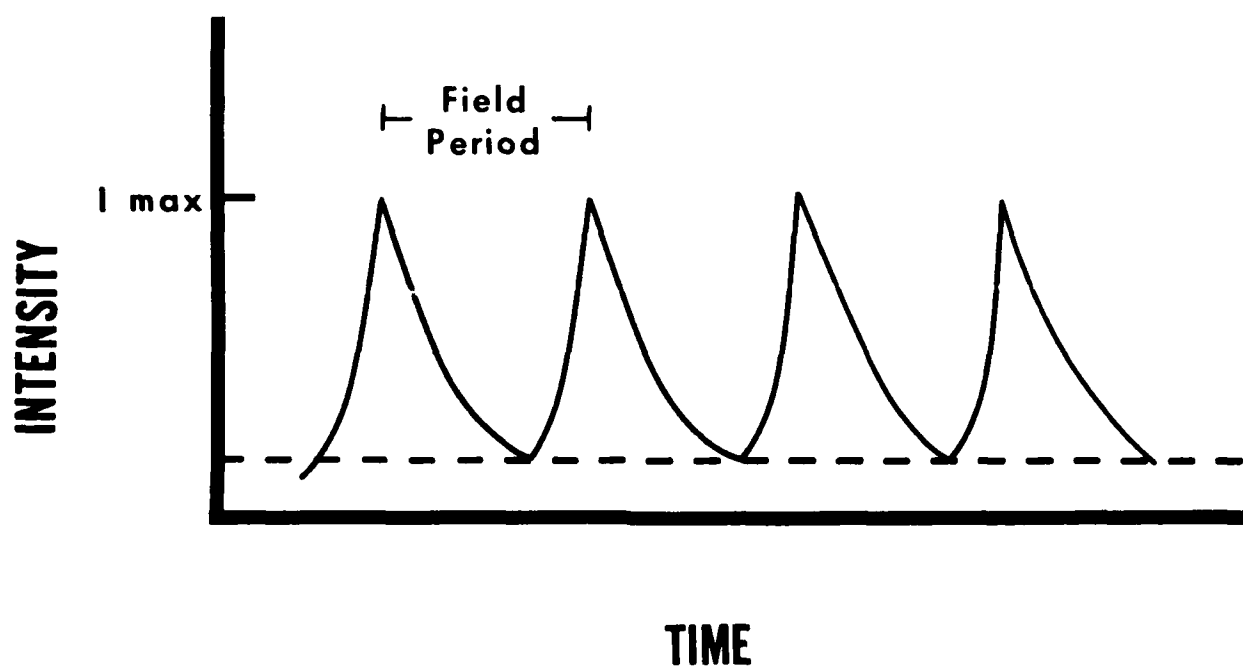
27

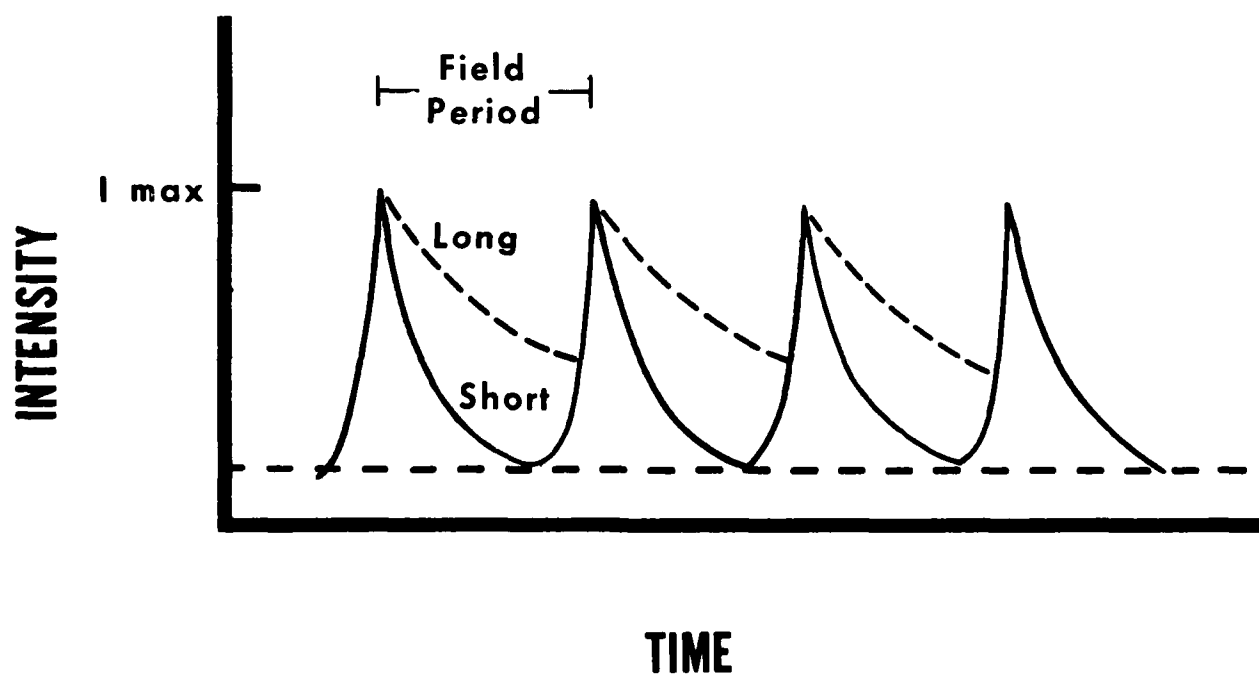FIGURE 14. Photometer output for single pixel under flat field condition.

FIGURE 15. Interaction of a short persistence phosphor and a long persistence phosphor with the field rate period.

$$I(t) = I_0 \exp\left((-2.3/\tau)(t-t_0)\right) + I_0 \exp\left((-2.3/\tau)(t-t_0+T)\right)$$

$$+ I_0 \exp\left((-2.3/\tau)(t-t_0+2T)\right) + \ldots \qquad \text{Eq. 11}$$

where T is the vertical frame period (33.33 msec) and t_0 is the time at which the particular pixel, located at point x'', y'' on the display image, is excited referenced to the beginning of the <u>last field scan</u>. The first term represents the contribution due to the most recent excitation. This is added to the residue of the preceding excitation, represented by the second term, and so on. A concise expression of Equation 11 can be written

$$I(t) = \sum_{N=0} I_0 \exp\left((-2.3/\tau)(t-t_0+NT)\right) \qquad \text{Eq. 12}$$

Using our assumption that the residual luminance after a period of 5τ following an excitation is negligible, then it is obvious that the expression in Equation 12 can be truncated after a finite number of terms which is dependent on the phosphor's persistence. For short phosphors ($\tau < 10$ μsec), 5τ or 50 μsec is three orders of magnitude smaller than the frame rate period, and the first term of Equation 12 will suffice. Even for long persistence phosphors ($\tau \approx 100$ msec), a period of 5τ, 500 msec, only requires fifteen terms.

IMAGING OF STATIC TARGETS

A static target will be defined here as one where there is no relative motion between the target and the sensor. The luminance profile of the target can be represented by a purely spatial function. The scanning of the target and the displaying of the video image of the target results in a luminance function on the display which is the luminance profile of the target after having been operated upon by the transfer functions of the detector, processing electronics, and display phosphor.

Since there are no temporal variations in the luminance of any point in the target, the intensity of any display pixel mapping onto that target point will vary temporally due only to the excitation rate (scan rate) and persistence of the phosphor. The intensity of the pixel as a function of time can be expressed by Equation 12 if the notation I_0 for a given pixel is replaced by the value $I_{x''}$ having the value which is dependent on the modulation present in the mapped target point and the aforementioned transfer functions. Such an expression may then be written as

$$I_{x''}(t) = \sum_{N=0} I_{0x''} \exp\left((-2.3/\tau)(t-t_0+NT)\right) \qquad \text{Eq. 13a}$$

This expression can be shown to be equivalent to

$$I_{x^{\prime\prime}}(t) = \exp\left((-2.3/\tau)(t-t_0)\right)\left(1/\left(1-\exp(-2.3T/\tau)\right)\right)$$ Eq. 13b

where $I_{x^{\prime\prime}}(t)$ is used to remind the reader that the maximum intensity of a pixel will depend upon which target point image is being studied.

This notation may be clarified by writing a pixel intensity function which incorporates the spatial variation in the display image of the target and the temporal characteristics of the scan rate and the phosphor's persistence. This function can be written as

$$I(t) = \frac{I_0}{2}\left[1+SIN(Kx^{\prime\prime}+\delta)\right]\sum_{N=0} \exp\left((-2.3/\tau)(t-t_0+NT)\right)$$ Eq. 14

where for analysis the target is chosen to be a sine wave pattern. The distance $x^{\prime\prime}$ is measured horizontally across the display, and δ represents a reference angle relative to the origin. A more in-depth discussion of the sinusoidal modulation term is provided in Appendix A.

In static imaging the display image maps point-for-point onto the target. Each image point maintains a luminous intensity value of $I_{0x^{\prime\prime}}$ in Equation 13. Because the temporal variation in the pixel intensity is due only to scan rate and phosphor persistence, it is common to use a detector whose integration time is several times greater than the electron beam scan period. This results in a detector output which represents the average intensity of the pixel over the integration period. A measure of the quality of a static image can be obtained by a rather straightforward technique requiring only a microphotometer and a modulated video source. The microphotometer is moved horizontally across the display in discrete steps, taking luminance measurements of the display modulation. Such a technique is more completely described by Virsu and Lehtiö (1975).

As discussed previously, the modulation transfer function (MTF) is most effective in describing the ability of a sensor/display system to "faithfully" reproduce target modulation. As seen in Figure 13, the low frequency content of a target is normally reproduced with no measurable loss in modulation. However, for higher spatial frequencies, severe modulation loss occurs due to the limited bandwidth of the display and the effects of spot size and backscatter from the display faceplate. The MTF obtained by use of sinusoidal patterns is a widely used figure-of-merit for CRT displays.

IMAGING OF DYNAMIC TARGETS

A dynamic target situation exists when there is relative motion between the target and the sensor. The three cases of relative target/sensor motion are (a) sensor at rest, target in motion, (b) target at rest, sensor in motion, and (c) both target and sensor in motion at different velocities. In the first and second cases cited, the magnitude of the relative target/sensor velocity

will be the target's speed or the sensor's speed, respectively. In the last case, the relative velocity will be the difference between the individual velocities of the target and sensor. In addition, within each of these cases, the direction of target travel across the sensor is important. For the type of sensor/display system discussed, vertical motion and horizontal motion must be examined separately. Psychophysical investigations by Williams and Borda (1964) have noted that optimum performance for target recognition on CRT displays occurs when target motion is vertical rather than horizontal. Noting that the analysis of horizontal and vertical motion is based on different principles, this preliminary analysis will be confined to horizontal motion only.

Turning again to the use of sinusoidal patterns to model image degradation, we will represent a horizontally moving target by a sinusoidal input with a continuous phase variation to the display phosphor. Varying the frequency of the sinusoidal input will result in varying spatial frequencies on the display. The continuously changing phase of the input modulation is responsible for the drifting of the sinusoidal pattern on the display. The rate of the drift will be directly proportional to the relative target/sensor velocity and can be changed by varying the rate of phase change on the input modulation. For a given pixel, location x'', its response to the modulation is given by the expression

$$I(t) = \frac{I_0}{2} \sum_{N=0} \left[1+SIN(Kx''-\omega NT+\delta)\right] \exp\left((-2.3/\tau)(t-t_0+NT)\right) \qquad \text{Eq. 15}$$

Introducing the spatial frequency variable (see Appendix) will change this expression to

$$I(t) = \frac{I_0}{2} \sum_{N=0} \left[1+SIN(2\pi Sx''-\omega NT+\delta)\right] \exp\left((-2.3/\tau)(t-t_0+NT)\right) \qquad \text{Eq. 16}$$

In both Equations 15 and 16, the term ω is related to the target's horizontal velocity by the geometry of the sensor's viewing system.

Equation 16 contains the following physical parameters: (ω) angular speed of bar pattern across display, (S) spatial frequency of bar pattern, (T) scan period of display, and (τ) persistence of phosphor. The angular speed (ω) can be more appropriately replaced in terms of the linear speed across the display in the following manner. A pixel responding to a spatial frequency S moving across the screen at a linear speed V is being driven at a temporal frequency of

$$f_t = SV. \qquad \text{Eq. 17}$$

Therefore,

$$\omega = 2\pi f_t = 2\pi SV. \qquad \text{Eq. 18}$$

31

This permits Equation 16 to be expressed as

$$I(t) = \frac{I_0}{2} \sum_{N=0} \left[1 + SIN(2\pi Sx'' - 2\pi SVNT + \delta) \right] \exp\left((-2.3/\tau)(t - t_0 + NT) \right) \qquad Eq.\ 19a$$

or

$$I(t) = \frac{I_0}{2} \sum_{N=0} \left[1 + SIN(2\pi S(x'' - VNT) + \delta) \right] \exp\left((-2.3/\tau)(t - t_0 + NT) \right) \qquad Eq.\ 19b$$

The signal expression of Equation 19b is valid, as in the static case, at any value of $t \geq t_0$.

IMAGE SMEAR

The imaging of moving targets on CRT displays can result in image quality degradation most apparent as smearing or blurring of the target's borders and loss of internal detail. While several studies have investigated effects of image motion (e.g., Farrell and Booth, 1975), none has satisfactorily investigated these effects in CRT displays. CRT displays, however, do have characteristics which degrade moving target image quality. The most dominant contributor to dynamic image degradation, which is sometimes called "smear," is the phosphor's persistence and its interaction with the sensor/display system's scan rate. The periodic nature of the CRT system's sampling process also introduces artifacts in both the spatial frequency content and the contrast of the image.

In order to facilitate our understanding of dynamic imagery, let us first review the CRT imaging of a static target. In this case an object point is repeatedly mapped to the same image point on the display during each sampling period. If the target itself has no temporal modulation, then the image point intensity will vary as depicted previously in Figures 14 and 15. The maximum intensity reached during each excitation will be a constant related to the luminance of the object point.

Noting that a stationary target with a sinusoidal varying intensity of frequency (f_t) would produce the same response at the detector as that of a target having a spatial frequency (S) and moving with a horizontal speed (V) equal to f_t/S, we shall therefore treat periodic dynamic targets as being equivalent to stationary targets undergoing periodic temporal variations in intensity. Since a CRT system has a characteristic sampling period (T), the phase difference on the modulated signal, $\Delta\phi$, associated with two successive samplings of a modulated target point can be expressed as:

$$\Delta\phi = 2\pi T/T_m \qquad \qquad Eq.\ 20$$

where T_m is the target intensity modulation period ($1/f_t$), and for the moment, $T_m > T$. Using the equivalence model, T_m can be replaced with

$$T_m = 1/SV \qquad\qquad \text{Eq. 21}$$

and Equation 20 can be rewritten as

$$\Delta\phi = 2\pi SVT \qquad\qquad \text{Eq. 22}$$

This phase difference is a determining factor of the image intensity profile, providing information regarding object to image transfer.

The object-to-image amplitude transfer is strongly influenced by the phosphor's persistence (τ). For example, if the persistence is of the order of T or greater, then the pixel intensity will contain a substantial residual phosphorescence from the previous excitation. The amount of residual phosphorescence depends upon the amplitude of the previous excitation and the ratio of τ to T. Thus, the object-to-image amplitude transfer is not significantly affected for $\tau \ll T$. However, for τ of the order of T or greater, the amplitude transfer degrades until, in the limit, no amplitude modulation can be perceived. For a given phosphor persistence (τ), we can examine worst case amplitude transfer by assuming that two successively sampled intensities are produced as a result of a 180^0 phase difference. Thus, the target's minimum intensity will be transferred as being the residual intensity of the maximum (I_0). The expression for the transferred minimum intensity, I_{min}, is

$$I_{min} = I_0 \left[\exp(-2.3T/\tau) + \exp\left(3(-2.3T/\tau)\right) +... \right] \qquad\qquad \text{Eq. 23}$$

The corresponding transferred maximum intensity, I_{max}, is

$$I_{max} = I_0 \left[1 + \exp\left(-2(2.3T/\tau) + \exp\ -4(2.3T/\tau)\right) +... \right] \qquad\qquad \text{Eq. 24}$$

Using Equations 23 and 24 and the definition for modulation which is

$$M = \frac{I_{max} - I_{min}}{I_{max} + I_{min}}, \qquad\qquad \text{Eq. 25}$$

the worst case amplitude transfer function for a given τ can be shown to be

$$M = \frac{1 - \exp(-2.3T/\tau)}{1 + \exp(-2.3T/\tau)} \ . \qquad\qquad \text{Eq. 26}$$

A plot of this function is given in Figure 16 for two values of T corresponding to the frame rate period of 33 msec and the field rate period of 17 msec. The field rate is included here in as much as optical systems often do not resolve a single pixel.

Included in Figure 16 are typical phosphors whose persistences vary from medium-short to very long (see Table 1). It can be seen that P43 shows no significant amplitude modulation loss. P1, a medium phosphor, shows some loss,

and the example of a long persistence phosphor, P28, exhibits extensive loss of modulation. Table 4 shows the maximum persistence allowable where a specific minimum modulation transfer is desired.
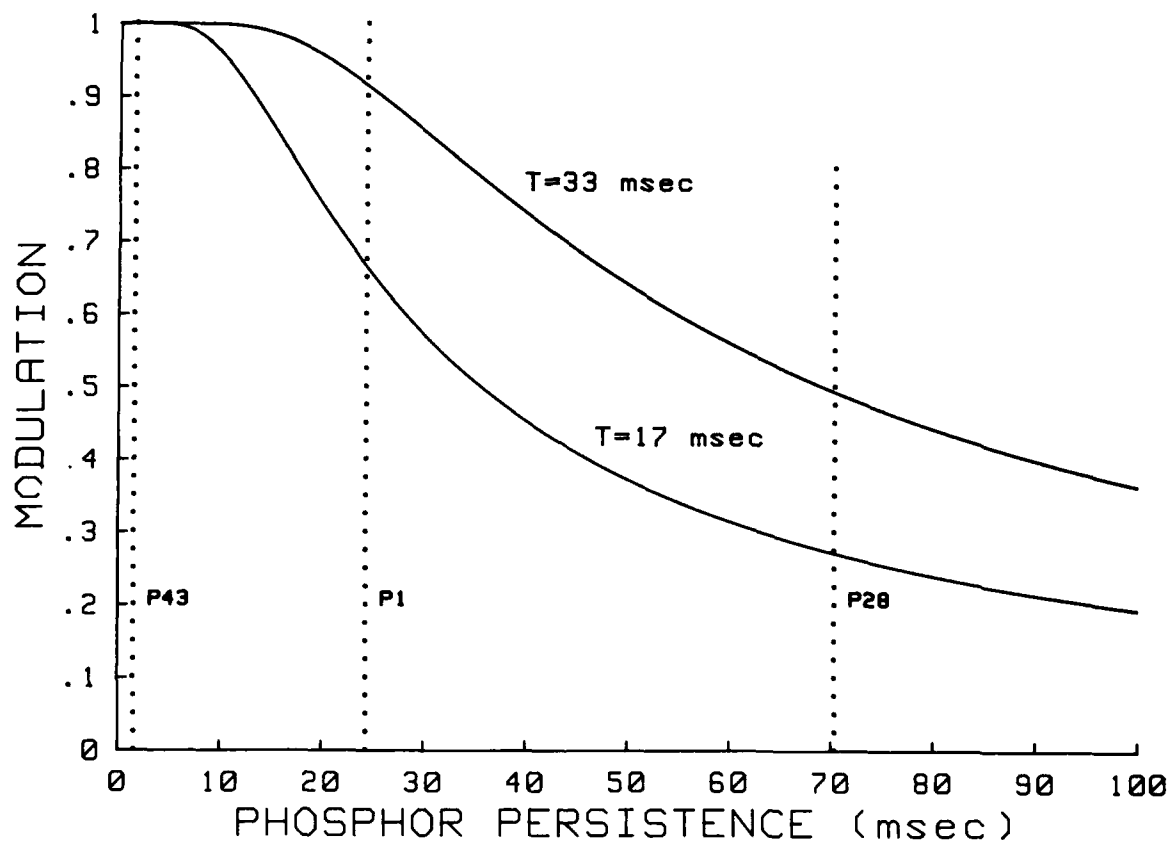

FIGURE 16. Worst case amplitude modulation transfer for the frame rate of 33 msec and the field rate of 17 msec.

TABLE 4

PERSISTENCE SELECTION

DESIRED MODULATION TRANSFER	MAXIMUM ALLOWABLE PERSISTENCE (10%) IN MSEC	
	T = 17 msec	T = 33 msec
.99	7.4	14.3
.98	8.5	16.5
.97	9.3	18.1
.96	10.0	19.5
.95	10.7	20.7
.90	13.3	25.8
.85	15.6	30.2
.80	17.8	34.5
.75	20.1	39.0

To examine amplitude modulation transfer for an arbitrary $\Delta\phi$, one needs to develop the expressions for the transferred minimum and maximum target intensities. The minimum intensity is a superposition of residual phosphorescences which can be written as

$$I_{min} = \frac{I_0}{2} \sum_{N=1} \left(1+SIN(3\pi/2-\omega NT)\right) exp(-2.3NT/\tau) \qquad \text{Eq. 27a}$$

$$= \frac{I_0}{2} \sum_{N-1} \left(1-COS(\omega NT)\right) exp(-2.3NT/\tau) \qquad \text{Eq. 27b}$$

This expression follows from Equation 15 by setting $Kx'' + \delta = 3\pi/2$ and $t = t_0$ where a minimum has appeared at the target. This causes the N=0 term to go to zero.

The transferred maximum intensity can be derived also from Equation 15 by setting $Kx'' + \delta = \pi/2$ and $t = t_0$ when a maximum has appeared at the target. In this case the N=0 term remains and takes on the value of I_0. The expression becomes

$$I_{max} = I_0 + \frac{I_0}{2} \sum_{N=1} \left(1+SIN(\pi/2-\omega NT)\right) exp(-2.3NT/\tau) \qquad \text{Eq. 28a}$$

$$= I_0 + \frac{I_0}{2} \sum_{N=1} \left(1+COS(\omega NT)\right) exp(-2.3NT/\tau) \qquad \text{Eq. 28b}$$

Using Equations 27b and 28b and the definition of modulation given in
Equation 25, we arrive at the expression

$$M = \frac{1 + \sum_{N=1} (\cos\omega NT)\exp(-2.3NT/\tau)}{1 + \sum_{N=1} \exp(-2.3NT/\tau)} \qquad \text{Eq. 29}$$

Using Equation 29 and sampling periods of T=17 msec and T=33 msec, Figures
17a and 17b show amplitude modulation transfer dependence on τ for various
values of $\Delta\phi$. If, in Equation 29, ω takes on the value of zero, corresponding
to a static target, the modulation transfer goes to one. This verifies that
this expression for modulation transfer represents the effects of velocity.

Figures 17 and 18 can be used as a guide for determining amplitude modu-
lation transfer of a specific phosphor, when $\Delta\phi$ is less than the worst case
condition.

The object-to-image frequency transfer of the equivalence model is dic-
tated by the previously mentioned function $\Delta\phi$. If the period between succes-
sive target samplings, which corresponds to a phase difference on the target's
modulation of $\Delta\phi = \frac{2\pi T}{T_m}$, is greater than π, then the model fails to represent
the true spatial frequency transfer.

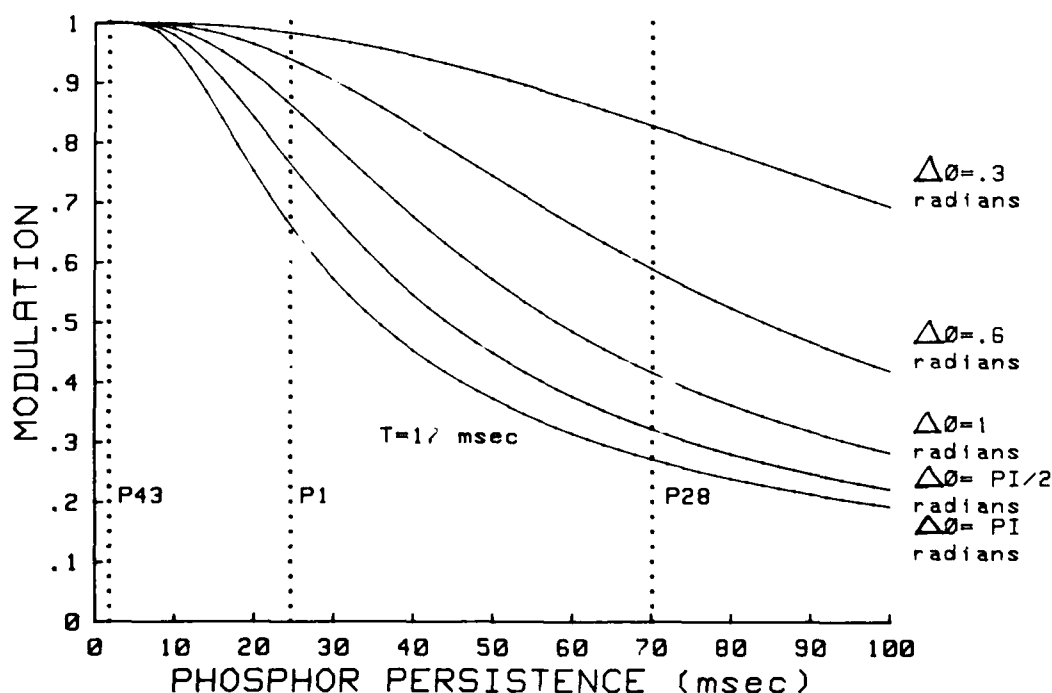

FIGURE 17. Modulation transfer for field rate
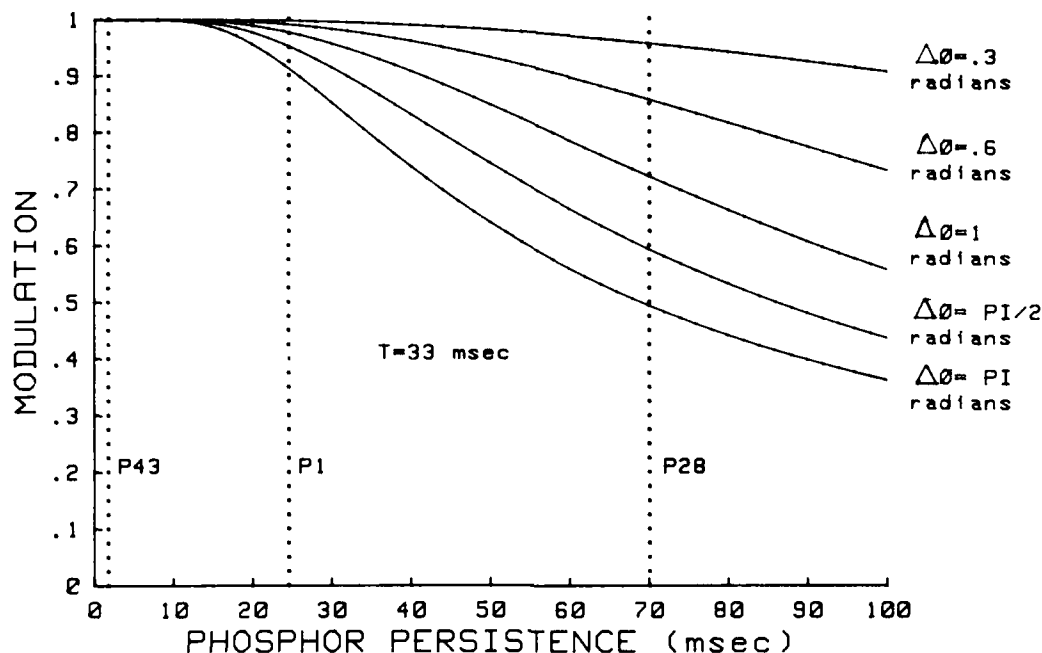T=17 msec for various values of $\Delta\phi$.

36

FIGURE 18. Modulation transfer for frame rate T=33 msec for various values of Δφ.

Thus, we will limit our discussion by considering sampling of target modulation with Δφ being less than π. Figure 19 shows amplitude modulation transfer for specific phosphors as a function of Δφ for T=33 msec. Phosphors included in the figure are P43 (τ=1.2 msec), P1 (τ=24 msec), and P28 (τ=70 msec). This figure is a plot of Equation 29 where ωNT is noted to be NΔφ.

Furthermore, we can examine the amplitude modulation transfer function for targets moving at various velocities by plotting modulation transfer as a function of spatial frequency (S) for a set of velocities using a specific phosphor. Figures 20 and 21 show such a family of curves for P28 and P1, respectively. The termination point of each curve is determined by the velocity and spatial frequency combination corresponding to a Δφ = π and defined by the limits of frequency reproduction. For Δφ>π the velocity information is distorted and visual perception dictates the object's apparent velocity.

At Δφ=π the apparent motion of a moving bar pattern on the display will reverse direction in a rather discontinuous manner. At Δφ=2π the bar pattern will appear stationary. At this point φ on the target's modulation is changing at a rate equal to 2π per vertical period. This results in the pixels

37
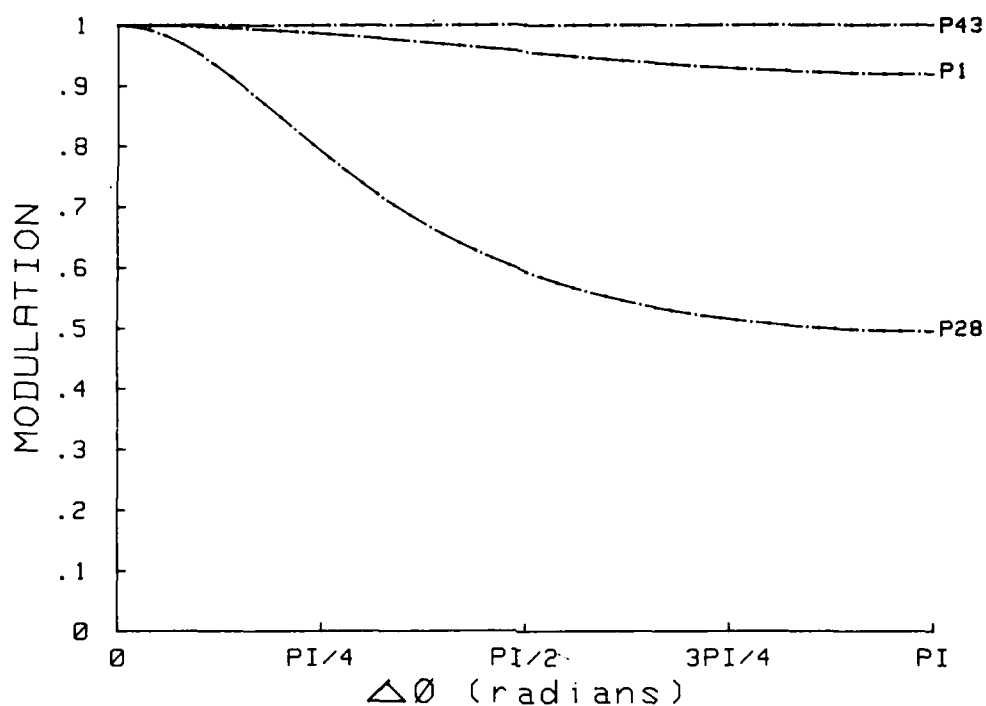
FIGURE 19. Amplitude modulation transfer for specific phosphors
as a function of Δφ.
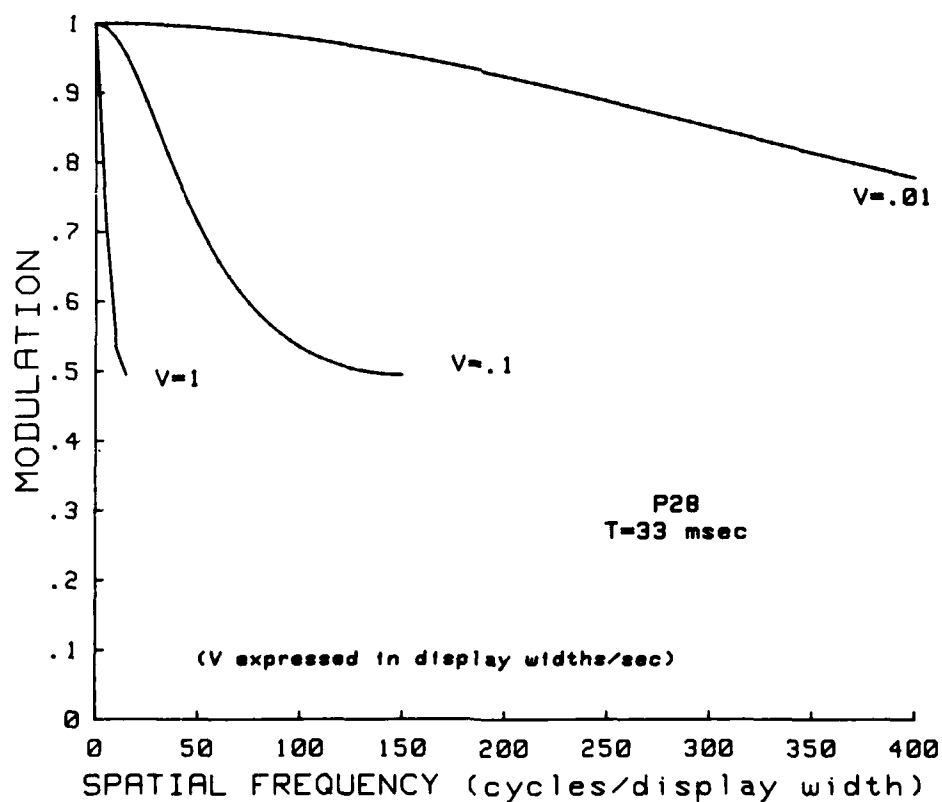
FIGURE 20. Modulation as a function of spatial frequency for selected
velocities for P28 phosphor at the frame rate of T=33 msec.

38
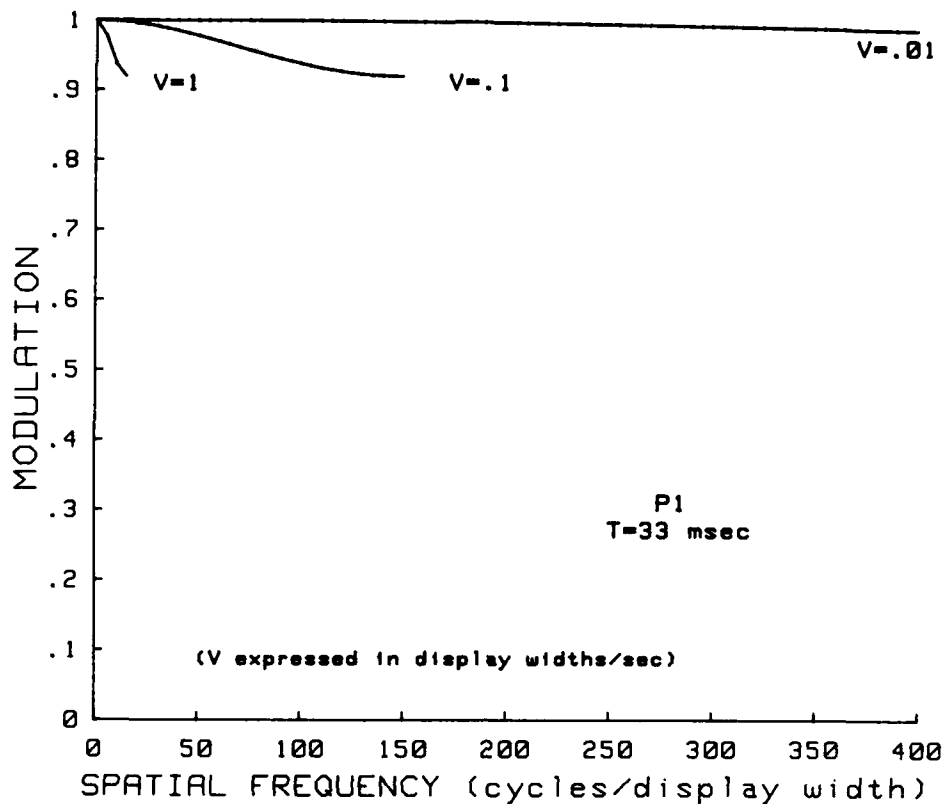
FIGURE 21. Modulation as a function of spatial frequency for selected velocities for P1 phosphor at the frame rate of T=33 msec.

continuously responding to the same phase point on the target. The target pattern image will appear to "freeze." For $\Delta\phi>2\pi$ the apparent motion will again reverse direction but this time rather smoothly. Thus, these display effects will repeat at intervals of 2π.

Another interesting effect of imaging moving bar targets is a tilting of the target bars on the display. This tilt is due to the change in the phase that occurs on the target during the horizontal scan period of ˜ 63 μsec. During this time the target modulation will have changed by an amount $\Delta\phi=2\pi SV(63\mu sec)$. Therefore the horizontal line scan immediately following will displace that phase point in the resulting display image. The amount of tilt will be proportional to the $\Delta\phi$ or the relative target/sensor velocity.

CONCLUSIONS

The derived expression for modulation transfer as a function of velocity and spatial frequency given in Equation 29 represents the interaction of velocity with scan rate and phosphor persistence. The graphs used to show this interaction provide comparative information between phosphors regarding modulation transfer.

Phosphor persistence as a contributor to loss of amplitude in the modulation transfer is examined. The sampling method used in CRT display systems is shown to result in distortion of velocity information. These analyses are based on the equivalence model, which is useful up to $\Delta\phi=\pi$. Using this information, it is possible to make comparative selection of phosphors for various applications.

The final transfer equation, Eq. 29, does not at this point include the spread of the electron beam spot or loss of modulation due to halation. Incorporation of these contributions to modulation loss would produce an expression which would allow more accurate calculations for the modulation transfer.

The second phase of this effort will be to incorporate into Equation 29 electron beam spot and halation factors as well as such problems as interlacing and phosphor non-linearity. In addition, the development of a measurement technique to quantify the amount of image degradation present on the display when moving targets are being imaged will be attempted.

REFERENCES

Cornsweet, T. N. 1970. *Visual Perception*. New York: Academic Press.

Farrell, R. J., and Booth, J. M. 1975. *Design handbook for imagery interpretation equipment*. Seattle, WA: Boeing Aerospace Company.

Goldmark, P. C. 1949. Brightness and contrast in television. *Electrical Engineering*. 68:170-175.

Hurford, W. L. 1967. Television interlace pairing: Its effect on detail response and its measurement. *IEEE Transactions on Broadcasting*. October.

Jenness, J. R., Jr., Eliot, W. A., and Ake, J. A. 1967. Intensity ripple in a raster generated by a Gaussian scanning spot. *Journal of the Society of Motion Picture and Television Engineers*. 76:544-550.

Keesee, R. L. 1976. *Prediction of modulation detectability thresholds for line-scan displays*. Wright-Patterson AFB, OH: Aerospace Medical Research Laboratory. AMRL-TR-76-38.

Larach, S., ed. 1965. *Photoelectronic materials and devices*. Princeton, NJ: D. Van Nostrand Co., Inc.

Leverenz, H. W. 1950. *An introduction to luminescence in solids*. New York: John Wiley and Sons, Inc.

Levi, L. 1968. *Applied optics, a guide to modern optical system design*. New York: John Wiley and Sons, Inc. Vol I.

Levi, L. 1968. *Applied optics, a guide to modern optical system design*. New York: John Wiley and Sons, Inc. Vol II.

Mertz, P., and Gray, F. 1934. A theory of scanning and its relation to characteristics of the transmitted signal in telephotography and television. *Bell Systems Technical Journal 13*.

Seyrafi, K. 1973. *Electro-optical systems analysis*. Los Angeles, CA: Electro-Optical Research Company.

Shires, D. 1979. *Phosphor decay and bandwidth measurements in image intensifiers*. 2nd International Conference on Low Light and Thermal Imaging, 3-5 April 1979, Nottingham, England. Stevenage, England: Institution of Electrical Engineers. IEE Conference Publication No. 173.

Spearnock, R. A. 1979. *Display measurements - can MTF analysis be used on matrix displays?* Wright-Patterson AFB, OH: Air Force Avionics Laboratory (AFAL/AAT). Technical Report AFAL-TR-79-1030.

Task, H. L. 1979. *An evaluation and comparison of several measures of image quality for television displays.* Wright-Patterson AFB, OH: Aerospace Medical Research Laboratory. AMRL-TR-79-7.

Virsu, V., and Lehtiö, P. K. 1975. A microphotometer for measuring luminance distributions on a CRT. *Behavior Research Methods and Instrumentation.* 7:29-33.

Westinghouse Electric Corporation. 1972. *Phosphor guide for industrial and military cathode-ray tubes.* Horseheads, NY: Westinghouse Electric Corp.

Westinghouse Electric Corporation. 1981. *Cathode-ray tubes.* Horseheads, NY: Westinghouse Electric Corporation.

Zworykin, V. K. and Morton, G. A. 1940. *Television - the electronics of image transmission.* New York: John Wiley and Sons, Inc.

Williams, H. L. and Borda, D. J. 1964. *Effects of selected parameters upon recognition of targets on a TV display.* Orlando, FL: Martin Marietta Corp. (OR 6072)

SELECTED BIBLIOGRAPHY

Fink, D. G. 1952. *Television engineering.* 2d ed. New York, NY: McGraw-Hill Publishing Co.

Hansen, G. L. 1969. *Introduction to solid-state television systems.* Inglewood Cliffs, NJ: Prentice-Hall, Inc.

Horn, J. E., and McCutcheon, M. J. 1970. Decay time of some image tube phosphors as a function of excitation time. *Proceedings of the Institute of Electrical and Electronics Engineers, Inc.* 58(4):592.

Larach, S., and Hardy, A. E. 1973. Cathode-ray tube phosphors: principles and applications. *Proceedings of the Institute of Electrical and Electronics Engineers, Inc.* 61(7):915.

Radio Corporation of America. 1974. *Electro-optics handbook.* Lancaster, PA: Radio Corporation of America.

APPENDIX

DESCRIPTION OF STATIC SINUSOIDAL LUMINANCE TARGET

Target information frequencies are usually expressed as "spatial frequencies." The term spatial frequency is defined as the number of cycles per unit linear measurement. Typical expressions for spatial frequency are cycles/target width, cycles/distance, cycles/display width, and sometimes, cycles/degree. For the static case, the choice of expression is not important since each expression varies from another by only a multiplicative constant. We will use the expression of cycles/distance. Such that

$$S = N/X \qquad \text{Eq. A-1}$$

where S is the spatial frequency,

   N is number of cycles, and

   X is linear distance on the target.

Assuming a mean luminance value of one, a sinusoidal luminance profile can be expressed as

$$L(x) = 1 + SIN(Kx+\delta) . \qquad \text{Eq. A-2.}$$

The wave number K, which is defined as

$$K = 2\pi/\lambda , \qquad \text{Eq. A-3}$$

is related to the spatial frequency, S, by the expression

$$S = 1/\lambda = \frac{K}{2\pi} \qquad \text{Eq. A-4}$$

where λ in Equations A-3 and A-4 is the cycle length expressed in distance units.

Therefore, a second expression for the luminance profile can be written as

$$L(x) = 1 + SIN(2\pi Sx +\delta), \qquad \text{Eq. A-5}$$

x being referenced to the left beginning edge of the target.

INITIAL DISTRIBUTION

Defense Technical Information Center
Cameron Station
Alexandria, VA 22314 (12)

Under Secretary of Defense for
  Research and Engineering
ATTN: Military Assistant for
  Medical and Life Sciences
Washington, DC 20301 (1)

Uniformed Services University
  of the Health Sciences
4301 Jones Bridge Road
Bethesda, MD 20014 (1)

Commander
US Army Medical Research and
  Development Command
ATTN: SGRD-RMS/Ms. Madigan
Fort Detrick
Frederick, MD 21701 (5)

Redstone Scientific Information
  Center
ATTN: DRDMI-TBD
US Army Missile R&D Command
Redstone Arsenal, AL 35809 (1)

US Army Yuma Proving Ground
Technical Library
Yuma, AZ 85364 (1)

US Army Aviation Engineering
  Flight Activity
ATTN: DAVTE-M (Technical Library)
Edwards AFB, CA 93523 (1)

US Army Combat Developments
  Experimentation Command
Technical Library
HQ, USACDEC
Box 22
Fort Ord, CA 93941 (1)

Aeromechanics Laboratory
US Army Research & Technology Labs
Ames Research Center, M/S 215-1
Moffett Field, CA 94035 (1)

Sixth United States Army
ATTN: SMA
Presidio of San Francisco,
California 94129 (1)

Director
Army Audiology & Speech Center
Walter Reed Army Medical Center
Forest Glen Section, Bldg 156
Washington, DC 20012 (1)

Harry Diamond Laboratories
Scientific & Technical Information
  Offices
2800 Powder Mill Road
Adelphi, MD 20783 (1)

US Army Ordnance Center & School
Library, Bldg 3071
ATTN: ATSL-DOSL
Aberdeen Proving Ground, MD
  21005 (1)

US Army Environmental Hygiene
  Agency Library, Bldg E2100
Aberdeen Proving Ground, MD
  21010 (1)

Technical Library
Chemical Systems Laboratory
Aberdeen Proving Ground, MD
  21010 (1)

US Army Materiel Systems
  Analysis Agency
ATTN: Reports Distribution
Aberdeen Proving Ground, MD
  21005 (1)

44

Commander
US Army Medical Research Institute
  of Chemical Defense
Aberdeen Proving Ground, MD
  21010   (1)

Commander
Naval Air Development Center
ATTN: Code 6022 (Mr. Brindle)
Warminster, PA 18974   (1)

Director
Ballistic Research Laboratory
ATTN: DRDAR-TSB-S (STINFO)
Aberdeen Proving Ground, MD
  21005   (2)

US Army Research & Development
  Technical Support Activity
Fort Monmouth, NJ 07703   (1)

Commander/Director
US Army Combat Surveillance &
  Target Acquisition Laboratory
ATTN: DELCS-D
Fort Monmouth, NJ 07703   (1)

US Army Avionics R&D Activity
ATTN: DAVAA-O
Fort Monmouth, NJ 07703   (1)

US Army White Sands Missile Range
Technical Library Division
White Sands Missile Range
New Mexico 88002   (1)

Chief
Benet Weapons Laboratory
LCWSL, USA ARRADCOM
ATTN: DRDAR-LCB-TL
Watervliet Arsenal
Watervliet, NY 12189   (1)

US Army Research & Technology Labs
Propulsion Laboratory MS 77-5
NASA Lewis Research Center
Cleveland, OH 44135   (1)

US Army Field Artillery School
  Library
Snow Hall, Room 16
Ft Sill, OK 73503   (1)

US Army Dugway Proving Ground
Technical Library
Bldg 5330
Dugway, UT 84022   (1)

US Army Materiel Development &
  Readiness Command
ATTN: DRCSG
5001 Eisenhower Avenue
Alexandria, VA 22333   (1)

US Army Foreign Science &
  Technology Center
ATTN: DRXST-IS1
220 7th St., NE
Charlottesville, VA 22901   (1)

Commander
US Army Training and Doctrine Command
ATTN: ATCD
Fort Monroe, VA 23651   (2)

Commander
US Army Training and Doctrine Command
ATTN: Surgeon
Fort Monroe, VA 23651   (1)

US Army Research & Technology Labs
Structures Laboratory Library
NASA Langley Research Center
Mail Stop 266
Hampton, VA 23665   (1)

Commander
10th Medical Laboratory
ATTN: DEHE (Audiologist)
APO New York 09180   (1)

Commander
US Army Natick R&D Laboratories
ATTN: Technical Librarian
Natick, MA 01760   (1)

Commander
US Army Troop Support & Aviation
 Materiel Readiness Command
ATTN: DRSTS-W
St. Louis, MO 63102   (1)

Commander
US Army Aviation R&D Command
ATTN: DRDAV-E
4300 Goodfellow Blvd
St. Louis, MO 63166   (1)

Director
US Army Human Engineering Laboratory
ATTN: Technical Library
Aberdeen Proving Ground, MD
 21005   (1)

Commander
US Army Aviation R&D Command
ATTN: Library
4300 Goodfellow Blvd
St. Louis, MO 63166   (1)

Commander
US Army Health Services Command
ATTN: Library
Fort Sam Houston, TX 78234   (1)

Commandant
US Army Academy of Health Sciences
ATTN: Library
Fort Sam Houston, TX 78234   (1)

Commander
US Army Airmobility Laboratory
ATTN: Library
Fort Eustis, VA 23604   (1)

Air University Library (AUL/LSE)
Maxwell AFB, AL 36112   (1)

US Air Force Flight Test Center
Technical Library, Stop 238
Edwards AFB, CA 93523   (1)

Command Surgeon
Rapid Deployment Joint Task Force
MacDill AFB, FL 33608   (1)

US Air Force Armament Development
 & Test Center
Technical Library
Eglin AFB, FL 32542   (1)

US Air Force Institute of Technology
 (AFIT/LDE)
Bldg 640, Area B
Wright-Patterson AFB, OH 45433   (1)

US Air Force Aerospace Medical
 Division
School of Aerospace Medicine
Aeromedical Library/TSK-4
Brooks AFB, TX 78235   (1)

Director of Professional Services
Office of The Surgeon General
Department of the Air Force
Washington, DC 20314   (1)

Human Engineering Division
Air Force Aerospace Medical
 Research Laboratory
ATTN: Technical Librarian
Wright-Patterson AFB, OH 45433   (1)

US Navy
Naval Weapons Center
Technical Library Division
Code 2333
China Lake, CA 93555   (1)

US Navy
Naval Aerospace Medical Institute
 Library
Bldg 1953, Code 012
Pensacola, FL 32508   (1)

US Navy
Naval Submarine Medical Research Lab
Medical Library, Naval Submarine Base
Box 900
Groton, CT 06340   (1)

Staff Officer, Aerospace Medicine
RAF Staff
British Embassy
3100 Massachusetts Avenue, N.W.
Washington, DC 20008   (1)

Director
Naval Biosciences Laboratory
Naval Supply Center, Bldg 844
Oakland, CA 94625   (1)

Naval Air Systems Command
Technical Library AIR 950D
RM 278 Jefferson Plaza II
Department of the Navy
Washington, DC 20361   (1)

US Navy
Naval Research Laboratory Library
Code 1433
Washington, DC 20375   (1)

US Navy
Naval Air Development Center
Technical Information Division
Technical Support Department
Warminster, PA 18974   (1)

Human Factors Engineering Division
Aircraft & Crew Systems Technology
  Directorate
Naval Air Development Center
Warminster, PA 18974   (1)

US Navy
Naval Research Laboratory Library
Shock & Vibration Information Center
Code 8404
Washington, DC 20375   (1)

Director of Biological & Medical
  Sciences Division
Office of Naval Research
800 N. Quincy Street
Arlington, VA 22217   (1)

Commanding Officer
Naval Medical R&D Command
National Naval Medical Center
Bethesda, MD 20014   (1)

Commanding Officer
Naval Biodynamics Laboratory
P.O. Box 29407
New Orleans, LA 70189   (1)

FAA Civil Aeromedical Institute
ATTN: Library
Box 25082
Oklahoma City, OK 73125   (1)

Department of Defence
R.A.N. Research Laboratory
P.O. Box 706
Darlinghurst, N.S.W. 2010
Australia   (1)

Canadian Society of Avn Med
c/o Academy of Medicine, Toronto
ATTN: Ms. Carmen King
288 Bloor Street West
Toronto, Ontario
M5S 1V8   (1)

COL F. Cadigan
DAO-AMLOUS B
Box 36, US Embassy
FPO New York 09510   (1)

DCIEM/SOAM
MAJ J. Soutendam (Ret.)
1133 Sheppard Avenue West
P.O. Box 2000
Downsview, Ontario
M3M 3B9   (1)

Dr. E. Hendler
Code 6003
Naval Air Development Center
Warminster, PA 18974   (1)

Commander
US Army Transportation School
ATTN: ATSP-TD-ST
Fort Eustis, VA 23604   (1)

47